

Article

Identification of Pyrrolo[2,3-d]pyrimidine-based Derivatives as Potent and Orally Effective Fms-like Tyrosine Receptor Kinase 3 (FLT3) Inhibitors for Treating Acute Myelogenous Leukemia

Xue Yuan, Yong Chen, Wanhua Zhang, Jun He, Lei Lei, Minghai Tang,
Jiang Liu, Muzhou Li, Caixia Dou, Tao Yang, Linyu Yang, Shengyong Yang,
Yuquan Wei, Aihua Peng, Ting Niu, Mingli Xiang, Haoyu Ye, and LiJuan Chen

J. Med. Chem., **Just Accepted Manuscript** • DOI: 10.1021/acs.jmedchem.9b00223 • Publication Date (Web): 02 Apr 2019

Downloaded from <http://pubs.acs.org> on April 3, 2019

Just Accepted

"Just Accepted" manuscripts have been peer-reviewed and accepted for publication. They are posted online prior to technical editing, formatting for publication and author proofing. The American Chemical Society provides "Just Accepted" as a service to the research community to expedite the dissemination of scientific material as soon as possible after acceptance. "Just Accepted" manuscripts appear in full in PDF format accompanied by an HTML abstract. "Just Accepted" manuscripts have been fully peer reviewed, but should not be considered the official version of record. They are citable by the Digital Object Identifier (DOI®). "Just Accepted" is an optional service offered to authors. Therefore, the "Just Accepted" Web site may not include all articles that will be published in the journal. After a manuscript is technically edited and formatted, it will be removed from the "Just Accepted" Web site and published as an ASAP article. Note that technical editing may introduce minor changes to the manuscript text and/or graphics which could affect content, and all legal disclaimers and ethical guidelines that apply to the journal pertain. ACS cannot be held responsible for errors or consequences arising from the use of information contained in these "Just Accepted" manuscripts.



ACS Publications

is published by the American Chemical Society, 1155 Sixteenth Street N.W.,
Washington, DC 20036

Published by American Chemical Society. Copyright © American Chemical Society.
However, no copyright claim is made to original U.S. Government works, or works
produced by employees of any Commonwealth realm Crown government in the course
of their duties.

1
2
3
4
5
6
7
8
9
10
11
12
13
14
15
16
17
18
19
20
21
22
23
24
25
26
27
28
29
30
31
32
33
34
35
36
37
38
39
40
41
42
43
44
45
46
47
48
49
50
51
52
53
54
55
56
57
58
59
60

	<p>Peng, Aihua; State Key Laboratory of Biotherapy/Collaborative Innovation Center of Biotherapy and Cancer Center, West China Hospital of Sichuan University</p> <p>Niu, Ting; Department of Hematology and Research Laboratory of Hematology, West China Hospital of Sichuan University</p> <p>Xiang, Mingli; State Key Laboratory of Biotherapy/Collaborative Innovation Center of Biotherapy and Cancer Center, West China Hospital of Sichuan University</p> <p>Ye, Haoyu; State Key Laboratory of Biotherapy and Cancer Center, West China Hospital, Sichuan University, and Collaborative Innovation Center for Biotherapy,</p> <p>Chen, LiJuan; State Key Laboratory of Biotherapy, West China Medical School</p>

SCHOLARONE™
Manuscripts

Identification of Pyrrolo[2,3-*d*]pyrimidine-based Derivatives as Potent and Orally Effective Fms-like Tyrosine Receptor Kinase 3 (FLT3) Inhibitors for Treating Acute Myelogenous Leukemia

Xue Yuan^{a,§}, Yong Chen^{a,§}, Wanhua Zhang^{b,§}, Jun He^{a,§}, Lei Lei^a, Minghai Tang^a, Jiang Liu^a, Muzhou Li^a, Caixia Dou^a, Tao Yang^a, Linyu Yang^a, Shengyong Yang^a, Yuquan Wei^a, Aihua Peng^a, Ting Niu^b, Mingli Xiang^a, Haoyu Ye^{a,*}, and Lijuan Chen^{a,*}

^a State Key Laboratory of Biotherapy and Cancer Center, National Clinical Research Center for Geriatrics; ^b Department of Hematology and Research Laboratory of Hematology, West China Hospital of Sichuan University, Chengdu, 610041, China.

§ These authors contributed equally and should be considered as co-first authors

Abstract

A series of pyrrolo[2,3-*d*]pyrimidine derivatives were prepared and optimized for cytotoxic activities against FLT3-ITD mutants cancer cells. Among them, compound **9u** possessed of nanomolar FLT3 inhibitory activity and subnanomolar inhibitory activities against MV4-11 and Molm-13 cells. It also showed excellent inhibitory activities in FLT3-ITD-D835V and FLT3-ITD-F691L cells which were resistant to quizartinib. Furthermore, **9u** exhibited over 40-fold selectivity toward FLT3 relative to c-Kit kinase, which might reduce myelosuppression toxicity. Cellular assays demonstrated that **9u** inhibited phosphorylated FLT3 and downstream signaling factors and also induced cell cycle arrest in G₀/G₁ stage and apoptosis in MV4-11 and Molm-13 cells. Oral administration of **9u** at 10 mg/kg could achieve rapid tumor

extinction in MV4-11 xenograft model and significantly inhibited the tumor growth in MOLM-13 xenograft model with TGI of 96% without obvious toxicity. Additionally, **9u** demonstrated high bioavailability (F=59.5%) and suitable eliminated half-life time ($T_{1/2}$ =2.06 h), suggesting that **9u** may be a potent candidate for treating AML.

Introduction

Acute myelogenous leukemia (AML) belongs to an invasive hematologic disorder characterized by blocked differentiation and deregulated proliferation of hematopoietic precursor cells^{1, 2}. Fms-like tyrosine receptor kinase 3 (FLT3) plays an essential role in hematopoiesis and leukemogenesis. The most frequent mutations in the FLT3 receptor gene are internal tandem duplications (FLT3-ITD), which account for approximately 25% in AML patients. Mutations in tyrosine kinase domain (FLT3-TKD) occupy close to 5%, mostly at the activation loop residue D835³. FLT3-ITD and FLT3-TKD mutations are activated, causing ligand-independent FLT3 receptor signaling transduction, and facilitating survival and proliferation of cytokine-independent AML cell, resulting in poor prognosis, higher recurrence, and low overall survival rate⁴⁻⁸.

Recently decades, plenty of FLT3 inhibitors have been studied and applied in clinical trials. The first-generation FLT3 inhibitors are multiple tyrosine receptor kinase inhibitors (RTKs), such as lestaurtinib⁹, midostaurin (PKC-412)¹⁰, and sorafenib¹¹, and could enhance anti-leukemia efficacy but lack specificity for FLT3, which may cause off-target toxicities. Midostaurin (PKC-412) blocks FLT3 autophosphorylation and induces growth arrest and apoptosis which has been approved by FDA for

treating newly diagnosed AML patients¹²⁻¹⁴. Quizartinib (AC220)³, as a second-generation specific FLT3 inhibitor, is in phase III clinical trial as monotherapy in refractory or relapsed AML patients (NCT02039726). However, the occurrence of FLT3-TKD mutations, most commonly at D835 and F691, is a mechanism of acquired resistance to quizartinib^{15, 16}. To overcome drug-resistance mutations, a novel, selective, and irreversible FLT3 inhibitor, FF-10101, which is in phase I clinical trial in US in refractory or relapsed AML patients (NCT03194685), has favorable therapeutic effects against AML cells with FLT3 mutations¹⁷. Although the first- and second-generation inhibitors achieve potent efficacy in AML, off-target toxicities such as myelosuppression caused by simultaneous inhibition of FLT3 and c-Kit¹⁸⁻²⁰, and FLT3-TKD mutations remain a big challenge for treating AML. For example, the selectivity margin of FLT3 vs c-Kit is only 10-fold, 3-fold and 20-fold for FF-10101, quizartinib and midostaurin respectively, which is in low scope of therapeutic window^{17, 21}. Thereby, improvement of the selectivity of FLT3 vs c-Kit could be a good strategy to decrease potential myelosuppression with maintenance of potent FLT3 inhibition effects.

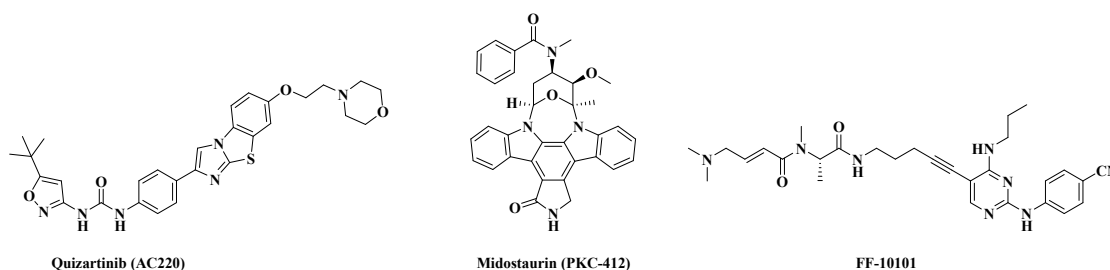


Figure 1. Illustration of representative FLT3 inhibitors.

Qingsong Liu group made great efforts focused on the development of FLT3 inhibitors in treating AML^{19, 22, 23}. They developed one FLT3 inhibitor

(CHMFL-FLT3-213) using pyrazolo[3,4-*d*]pyrimidine as core pharmacophore using a structure-guided drug design methodology. CHMFL-FLT3-213 potently interfered FLT3-ITD mediated signal pathways and showed highly potent anti-tumor effect in FLT3-ITD positive AML¹⁶. However, the low selectivity scope of FLT3 vs c-Kit (0.9-fold) and relatively low bioavailability may affect effectiveness in clinical trial. On the basis of their studies, we further studied the binding mode of CHMFL-FLT3-213 with FLT3 kinase, and found that pyrazolo[3,4-*d*]pyrimidine of CHMFL-FLT3-213 can be replaced by pyrrolo[2,3-*d*]pyrimidine. The positions of urea-linked benzene ring and ethylmorpholine can be exchanged while the binding capacity with FLT3 kinase can be retained. Hence, we adopted pyrrolo[2,3-*d*]pyrimidine as the core skeleton and simplified functional group with retained key functional group and tried to improve the selectivity of FLT3 vs c-Kit and bioavailability. Numerous compounds were designed, prepared, and evaluated for biochemical effects. Among them, **9u** showed efficient inhibitory effects in FLT3-ITD positive cancer cells and two secondary mutation transformed BaF3 cells including FLT3-ITD-D835V and FLT3-ITD-F691L (Figure 2). **9u** had higher selectivity toward FLT3 relative to c-Kit than quizartinib and CHMFL-FLT3-213. More importantly, **9u** possessed good pharmacokinetics and favorable safety profiles. **9u** could achieve complete tumor remission at low dosage without obvious observed toxicities. All the results indicated that **9u** was an excellent drug candidate for treating AML.

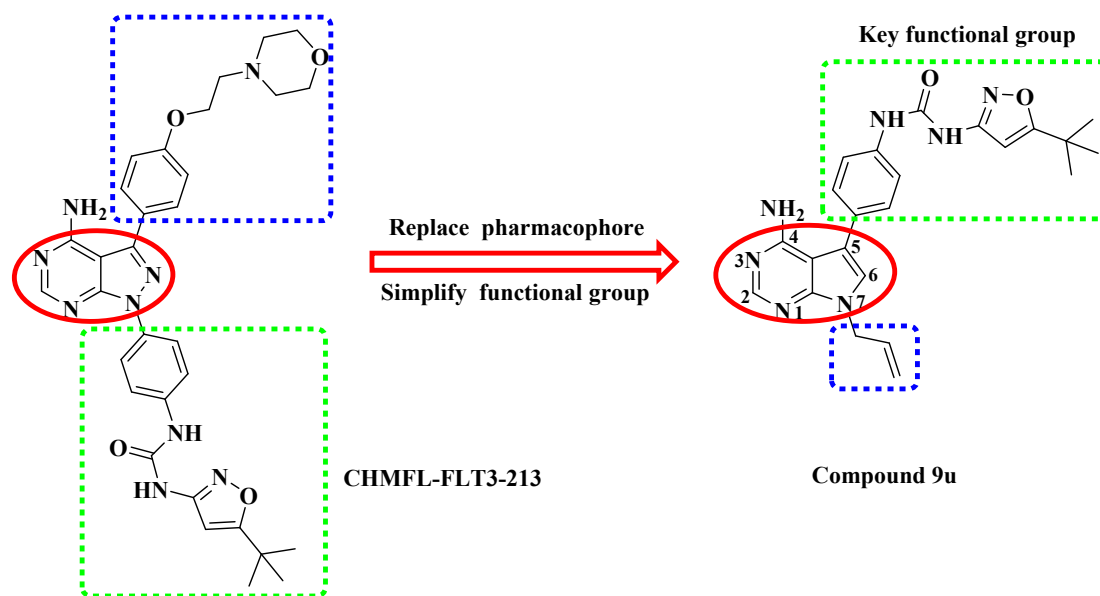


Figure 2. Structural explanation of development of compound **9u**.

Results and Discussions

Rational Strategy Based on Computer Aided Design

We first investigated the similarities and differences of binding mode between compound **9a** with pyrrolo[2,3-*d*]pyrimidine and reference compound CHMFL-FLT3-213 with FLT3 kinase. As illustrated in Figure 3A, CHMFL-FLT3-213 formed three canonical hydrogen bonds between the urea moiety with Glu661 and Asp829 residues. Two hydrogen bonds formed between the amino and pyrimidine with Cys694 and Cys695, and pyrazol didn't form hydrogen bonds with ambient amino acid residues. The hydrophobic pocket was occupied by the tert-butyl substituted isoxazole. When urea-linked benzene ring moiety was moved to C-5 position and ethylmorpholine was moved to N-7 position of pyrrole, compound **9a** adopted a similar docking mode with FLT3 kinase (Figure 3B). **9a** still formed three canonical hydrogen bonds by the urea moiety with the residues of Glu661 and Asp829. Amino of pyrimidine formed hydrogen with Glu692 and π - π stacking was

1
2
3
4 formed between the linking phenyl with Phe691 and Phe830 residues. When
5
6 CHMFL-FLT3-213 and **9a** were placed together, they adopted highly similar
7
8 alignment and were well embedded in the pocket (Figure 3C). Inspired by the
9
10 encouraging design outcomes, we continued to design and synthesize a series of
11
12 compounds and evaluate their biochemical activities in vitro and in vivo.
13
14
15
16
17
18
19
20
21
22
23
24
25
26
27
28
29
30
31
32
33
34
35
36
37
38
39
40
41
42
43
44
45
46
47
48
49
50
51
52
53
54
55
56
57
58
59
60

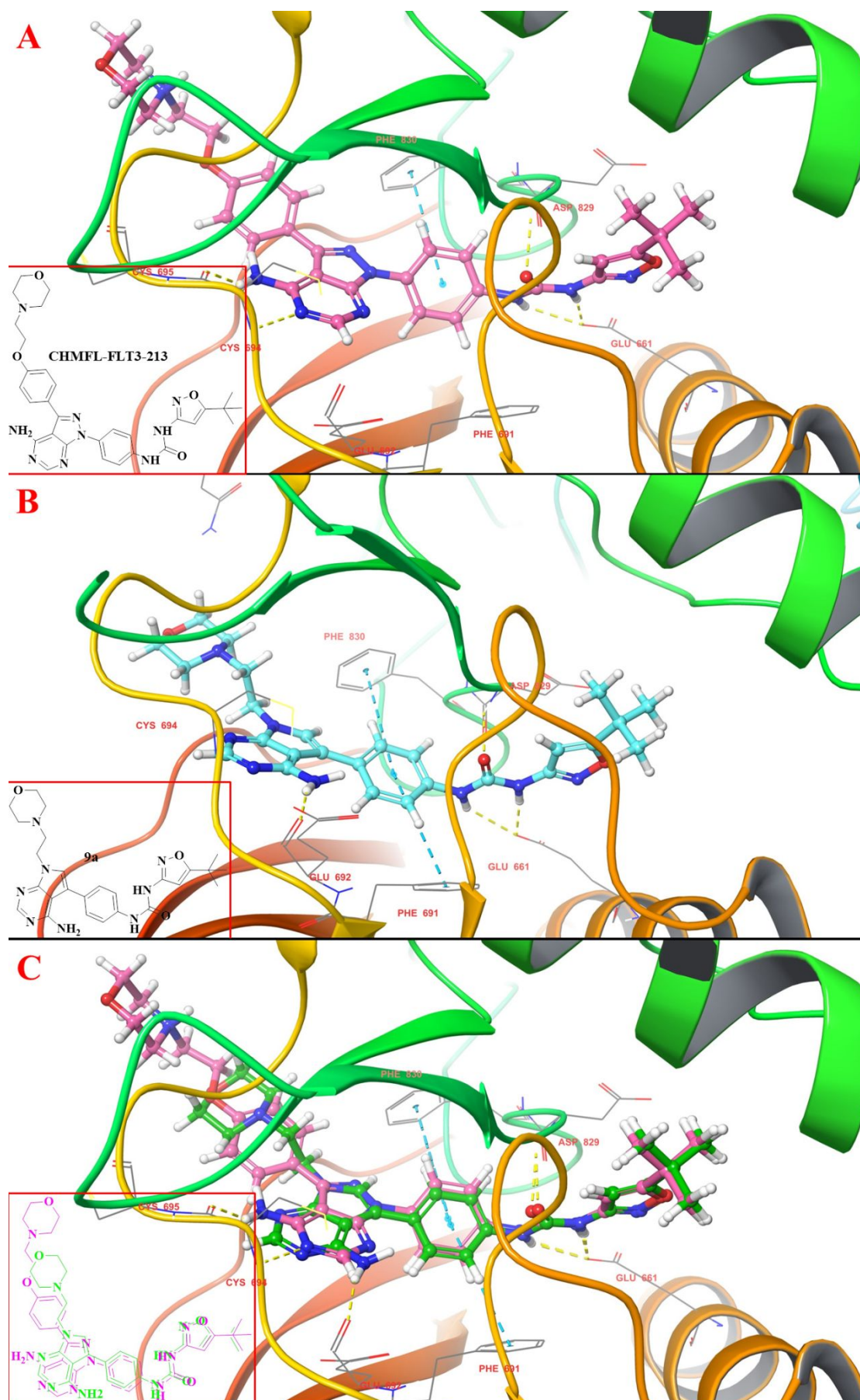


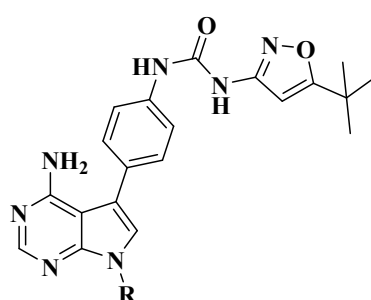
Figure 3. Docking model using FLT3 kinase (PDB code: 4XUF). (A) CHMFL-FLT3-213 was docked into the FLT3 kinase. (B) **9a** was docked into the FLT3 kinase. (C) Alignment of CHMFL-FLT3-213 and **9a** into the FLT3 kinase.

In Vitro Cell Growth Inhibitory Effects and Enzymatic Inhibitory Activities

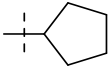
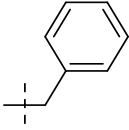
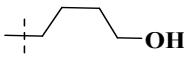
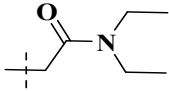
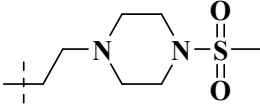
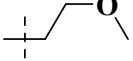
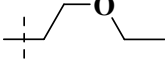
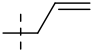
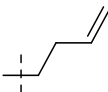
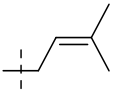
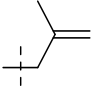
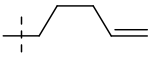
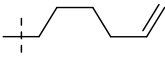
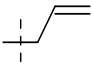
against FLT3 Kinase. The introduction of 3-amino-5-tert-butylisoxazole group to aniline could improve the potency for FLT3^{3, 16, 24}. Thus we attempted to keep the key functional group and compounds **9a-ae** were synthesized. MV4-11 and Molm-13 cells are both FLT3-ITD positive cells, which can reflect the antitumor activities of compounds against FLT3 mutant cells. Thereby we primarily evaluated the inhibitory activities of compounds **9a-ae** in MV4-11 and Molm-13 cells. As expected, all the compounds showed potent inhibitory activities against MV4-11 and Molm-13 cells and the IC₅₀ values were below 10 nM (Table 1). **9a** with ethylmorpholine showed comparable inhibitory activity to quizartinib. **9f** with extended carbon chain of morpholine enhanced the inhibitory activity with IC₅₀ values of 0.069 nM and 0.193nM in MV4-11 and Molm-13 cells respectively. Introduction with large substituents at N-7 position such as benzyl (**9o**), cyclopentane (**9n**) and 1-ethyl-4-(methylsulfonyl)piperazine (**9r**) significantly decreased the inhibitory effects. Interestingly, compounds with short nonsubstitutive aliphatic chains, such as **9g-k**, **9p**, **9s-v**, exhibited stronger inhibitory activities at the subnanomolar level or even the picomole level. Surprisingly, **9b** without substitution at N-7 position showed the strongest inhibitory effect with IC₅₀ < 1 pM against Molm-13. These compounds were further evaluated IC₅₀ values against FLT3 kinase. Several compounds showed potent

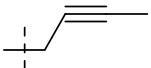
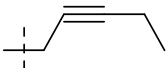
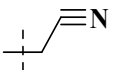
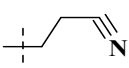
inhibitory activities against FLT3 with average IC_{50} below 10 nM and displayed comparable effects with quizartinib ($IC_{50} = 7.4$ nM)²⁵. These results were in accordance with our previous rational drug design and these potent compounds should be further evaluated to obtain the optimal drug candidate.

Table 1. IC_{50} Values of Compounds **9a-e** in MV4-11, Molm-13, and FLT3 Kinase and Quizartinib as Positive Control



Compd	R	$IC_{50} \pm SD^a$, nM		IC_{50}^b , nM
		MV4-11	Molm-13	FLT3
9a		0.329 ± 0.035	1.153 ± 0.096	20
9b	H	0.043 ± 0.007	< 0.001	6
9c	Boc	0.107 ± 0.010	0.081 ± 0.025	25
9d		2.536 ± 0.193	4.435 ± 0.364	ND ^c
9e		1.751 ± 0.010	2.56 ± 0.513	9
9f		0.069 ± 0.015	0.193 ± 0.027	9
9g		0.152 ± 0.010	0.134 ± 0.016	17
9h	Methyl	0.311 ± 0.084	0.014 ± 0.003	7

9i	Ethyl	0.476 ± 0.057	0.144 ± 0.017	7
9j	Isopropyl	0.100 ± 0.045	0.971 ± 0.121	20
9k	Propyl	0.403 ± 0.091	0.736 ± 0.010	15
9l	n-butyl	2.179 ± 0.281	1.425 ± 0.306	34
9m	n-hexyl	5.133 ± 2.010	3.771 ± 0.468	105
9n		2.160 ± 0.063	1.511 ± 0.038	32
9o		1.756 ± 0.198	2.495 ± 0.225	86
9p		0.876 ± 0.131	0.140 ± 0.001	16
9q		1.734 ± 0.049	1.946 ± 0.052	31
9r		14.173 ± 0.620	10.601 ± 0.110	26
9s		0.149 ± 0.042	0.049 ± 0.010	21
9t		1.468 ± 0.022	0.117 ± 0.010	37
9u		0.089 ± 0.001	0.022 ± 0.003	7
9v		1.753 ± 0.134	1.061 ± 0.055	38
9w		10.325 ± 1.255	2.767 ± 0.116	113
9x		1.746 ± 0.219	1.025 ± 0.097	30
9y		2.940 ± 0.282	2.222 ± 0.184	69
9z		1.788 ± 0.615	2.855 ± 0.016	70
9aa		0.602 ± 0.068	0.262 ± 0.041	13

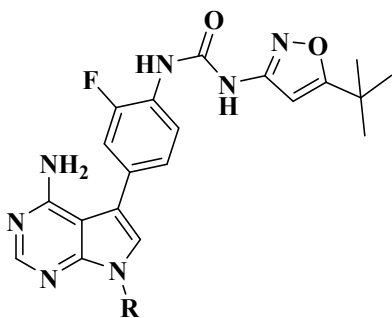
9ab		3.923 ± 0.384	1.145 ± 0.072	26
9ac		5.842 ± 0.221	2.046 ± 0.210	64
9ad		0.032 ± 0.007	0.038 ± 0.010	9
9ae		0.376 ± 0.041	0.520 ± 0.030	6
quizartinib		0.452 ± 0.177	1.885 ± 0.220	7.4

^a IC₅₀, compound concentration required to inhibit tumor cell proliferation by 50%, data are expressed as the mean \pm SD from the dose-response curves of at least three independent experiments. ^b IC₅₀ values for enzymatic inhibition of FLT3 kinase; data are expressed from the dose-response curves of at least two independent experiments. ^c ND, not detected.

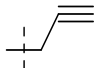
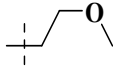
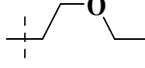
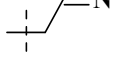
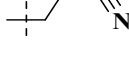
Although compound **9b** showed potent anti-proliferative activity against Molm-13 with IC₅₀ < 1 pM, which was more than 100-times active than quizartinib. However, **9b** showed unsatisfactory bioavailability and anti-tumor activity in vivo (data was not shown). The bioavailability and anti-tumor activity of other two promising compounds **9a** and **9f** in vivo were also unsatisfactory (data was not shown). Very luckily, **9u** with allylic substitution obtained satisfactory bioavailability and anti-proliferation effect both in MV4-11 and Molm-13 cells (Table 1). It is well known that introduction of key functional groups (such as halogen atom) is an important structural modification strategy to improve metabolic stability and bioavailability of lead compounds²⁶. We attempted to introduce F atom to C-3 position of phenyl in selected compounds and **13a-h** were synthesized and evaluated for inhibitory activities in MV4-11 and Molm-13 cells. The data were illustrated in

Table 2. Although F-substitued analogues maintained potent inhibitory activities in MV4-11 and Molm-13 cells, they decreased efficacy in comparision with corresponding analogues without F atom. Worsemore, F-substitued analogues decreased inhibitory activities against FLT3 kinase except for **13a** with IC₅₀ of 4 nM. Since wild-type FLT3 is essential for the proliferation of normal primitive hematopoietic cells²⁷, all the compounds were further evaluated the inhibitory activities in RS4;11 (acute lymphoblastic leukemia, FLT3 wt) and HL-60 (promyelocytic leukemia cell, FLT3 wt). These compounds showed very weak inhibitory activities against RS4;11 and HL-60, and the IC₅₀ values were > 1000 nM (Table S2 and S3), indicating that these compounds possessed of excellent selectivity between FLT3 wt and FLT3-ITD mutants (MV4-11, Molm-13).

Table 2. IC₅₀ Values of Compounds **13a-h** in MV4-11, Molm-13, and FLT3 Kinase and Quizartinib as Positive Control



Compd	R	IC ₅₀ ± SD ^a , nM		IC ₅₀ ^b , nM
		MV4-11	Molm-13	FLT3
13a	H	0.131 ± 0.035	0.007 ± 0.001	4
13b		2.336 ± 0.022	0.650 ± 0.038	17
13c		3.223 ± 0.067	1.450 ± 0.050	51

13d		0.434 ± 0.084	0.389 ± 0.047	46
13e		1.977 ± 0.100	0.580 ± 0.010	32
13f		1.343 ± 0.157	1.550 ± 0.180	49
13g		0.422 ± 0.057	0.730 ± 0.120	19
13h		2.208 ± 0.298	2.330 ± 0.190	22
quizartinib		0.452 ± 0.177	1.885 ± 0.220	7.4

^a IC₅₀, compound concentration required to inhibit tumor cell proliferation by 50%, data are expressed as the mean \pm SD from the dose-response curves of at least three independent experiments. ^b IC₅₀ values for enzymatic inhibition of FLT3 kinase; data are expressed from the dose-response curves of at least two independent experiments.

Patients with FLT3-ITD mutations which relapsed while treated with quizartinib usually had point mutations in activation loop (most frequently at D835) or “gatekeeper” domain²⁸. F691L is a hotspot for drug resistance to FLT3 inhibitors which situated at the “gatekeeper” location in FLT3 kinase^{16, 29}. These secondary mutations conferring resistance in kinase domain will pose a significant clinical challenge, which prompted us to identify new FLT3 inhibitors against FLT3 resistant variants³⁰. FLT3-ITD, FLT3-ITD-F691L and D835V transformed BaF3 cells were established to evaluate inhibitory activities of all the compounds. On the basis of the characteristics of inhibitory activities in MV4-11 and Molm-13 cells and IC₅₀ values of FLT3 kinase of the above compounds, all the compounds were further evaluated the inhibitory activities against BaF3-FLT3-ITD cell. As shown in Table 3, all the

compounds strongly inhibited proliferation of BaF3-FLT3-ITD with IC₅₀ values at the nanomolar level, but showed great difference between BaF3-FLT3-ITD-F691L and BaF3-FLT3-ITD-D835V. Most compounds still exhibited potent inhibitory effects against these two mutational cells which were resistant to quizartinib and a majority of these compounds were below 100 nM (IC₅₀). **9b**, **9j**, **9p**, **9u**, **9aa**, **9ad**, and **13a** showed considerable and equivalent potent effects against FLT3-ITD-F691L and FLT3-ITD-D835V cells. Conclusion can be drawn that these compounds could overcome two crucial point mutations which conferred resistance to quizartinib. Considering of cytotoxicity and FLT3 kinase assay, **9b**, **9j**, **9p**, **9u**, **9aa**, **9ad**, and **13a** were further selected out and evaluated their bioavailability in SD rats.

Table 3. IC₅₀ Values of Compounds **9a-ae** and **13a-h** against FLT3 Mutants Transformed BaF3 Cells and Quizartinib as Positive Control

Compd	IC ₅₀ ±SD ^a , nM		
	BaF3-ITD	BaF3-ITD-D835V	BaF3-ITD-F691L
9a	1.07 ± 0.05	52.38 ± 1.66	34.81 ± 6.75
9b	0.16 ± 0.04	4.83 ± 0.25	2.35 ± 0.40
9c	1.28 ± 0.19	12.39 ± 1.26	8.92 ± 1.18
9d	8.95 ± 0.81	385.4 ± 82.2	> 500
9e	8.67 ± 0.32	155.67 ± 9.54	> 200
9f	0.99 ± 0.10	61.84 ± 8.11	32.12 ± 3.52
9g	1.62 ± 0.15	170.23 ± 12.40	85.02 ± 8.00
9h	1.44 ± 0.09	46.25 ± 3.05	27.92 ± 0.71
9i	0.92 ± 0.13	23.09 ± 2.31	28.53 ± 3.93
9j	5.30 ± 0.57	12.19 ± 1.86	12.56 ± 0.52
9k	2.72 ± 0.24	41.49 ± 2.69	72.09 ± 3.96

9l	5.69 ± 0.80	111.5 ± 0.2	208.7 ± 31.7
9m	20.71 ± 1.98	187.0 ± 11.9	252.7 ± 27.8
9n	7.25 ± 0.79	36.80 ± 5.57	90.87 ± 0.83
9o	8.45 ± 0.07	95.40 ± 6.43	133.5 ± 22.3
9p	1.73 ± 0.03	14.74 ± 0.91	13.63 ± 1.82
9q	3.10 ± 0.47	28.50 ± 1.86	28.23 ± 4.31
9r	3.59 ± 0.24	166.5 ± 4.4	85.99 ± 13.22
9s	0.95 ± 0.12	50.14 ± 1.89	28.65 ± 0.70
9t	3.21 ± 0.78	173.0 ± 5.2	98.6 ± 12.1
9u	0.92 ± 0.01	20.71 ± 2.32	12.99 ± 0.87
9v	4.92 ± 1.04	175.6 ± 11.4	91.8 ± 0.7
9w	8.67 ± 0.29	305.3 ± 31.7	216.5 ± 6.0
9x	5.09 ± 0.96	93.7 ± 9.3	57.79 ± 8.30
9y	5.95 ± 0.18	139.8 ± 10.2	200.3 ± 5.7
9z	6.06 ± 0.72	185.3 ± 8.5	228.1 ± 16.9
9aa	1.66 ± 0.04	21.15 ± 1.09	13.88 ± 0.77
9ab	6.18 ± 0.69	86.43 ± 5.68	51.17 ± 6.26
9ac	8.65 ± 0.02	361.1 ± 21.3	147.9 ± 6.8
9ad	0.97 ± 0.07	9.17 ± 0.48	3.61 ± 0.01
9ae	1.60 ± 0.06	24.64 ± 0.44	19.60 ± 1.33
13a	0.25 ± 0.04	18.01 ± 0.87	10.71 ± 1.48
13b	3.04 ± 0.26	51.85 ± 5.17	82.43 ± 4.92
13c	5.41 ± 0.53	84.41 ± 4.24	50.25 ± 2.16
13d	2.48 ± 0.16	102.5 ± 5.7	16.08 ± 0.86
13e	5.57 ± 0.27	69.70 ± 5.97	39.39 ± 2.57
13f	4.60 ± 0.33	55.37 ± 4.21	42.66 ± 2.76
13g	1.27 ± 0.09	86.69 ± 1.24	9.84 ± 0.58
13h	4.26 ± 0.33	111.5 ± 10.9	31.46 ± 1.58
quizartinib	4.94 ± 0.20	> 1000	> 1000

^a IC₅₀, compound concentration required to inhibit tumor cell proliferation by 50%, data are expressed as the mean ± SD from the dose-response curves of at least three independent experiments.

As shown in Table 4, **13a** with F-substitution showed poor pharmacokinetic (PK) properties than **9b**, suggesting that halogen contributed worse effect to PK properties. **9p** with hydroxyl group significantly promoted the clearance of drug. Compound **9ad** wasn't further explored due to its high clearance rate and low bioavailability. Among them, compound **9u** demonstrated excellent PK properties with low clearance (1.22 L/h/kg), reasonable half-life time (2.06 h), and highest oral exposure (59.5%). These PK properties showed strong correlation with bioavailability predicted by swissADME tool (Figure S1 and S2)³¹.

Table 4. Oral Pharmacokinetic Study of the Selected Compounds in SD Rats^a

Parameter	9 b	9j	9p	9u	9aa	9ad	13a
T_{max} (h)	0.28	0.50	0.31	0.75	0.83	0.44	0.88
T_{1/2} (h)	6.22	4.22	2.77	2.06	2.78	3.7	2.54
CL (L/h/kg)	0.89	15.31	48.07	1.22	1.70	9.17	3.38
F (%)	22.5	12.1	9.8	59.5	40.0	11.2	25.6

^a Dosage, 5 mg/kg po; T_{max}, time for peak concentration; T_{1/2}, elimination half-life period; V_{ss}, distribution volume; CL, plasma clearance; F (%), percent oral bioavailability.

Kinase Selectivity Profiling of Compound 9u. To further understand the selectivity of compound **9u**, we then evaluated its wide kinome selectivity profile. The results

indicated that compound **9u** possessed a relatively good selectivity in a panel of more than 400 kinases and mutants at 100 nM (Table S1). The *S* (10) selectivity score, which is calculated by dividing the number of nonmutant kinases which are $\leq 10\%$ of control can be determined by the total number of nonmutant kinases³². From the nonmutant kinases there were 38 hits, giving the selectivity of 0.17 (Figure 4). Because receptor tyrosine kinase inhibitors usually target many other targets which share homologous sequences. Thereby the inhibitory activities of **9u** against hit targets were further evaluated the IC_{50} values and the data were shown in Table S4. Most importantly, **9u** showed good selectivity of FLT3 to c-Kit, and its selectivity range of FLT3 vs c-Kit was > 40 -fold (FLT3, $IC_{50} = 7$ nM; c-Kit, $IC_{50} > 300$ nM), much better than quizartinib and CHMFL-FLT3-213, indicating that **9u** possessed of better safety window. Additionally, Hck, Ret, Lyn, Lck, Mer, Met, and Tie2 kinases have been proved as promising targets for treating leukemia³³⁻³⁹. Fibroblast growth factor receptor (FGFR) is also overexpressed in leukemia cells and could be one promising druggable target for treating leukemia⁴⁰⁻⁴². **9u** also strongly inhibited PDGFR α mutants at D842V and V561D and Abl (T315I), which might overcome imatinib-resistant mutants^{43, 44}.

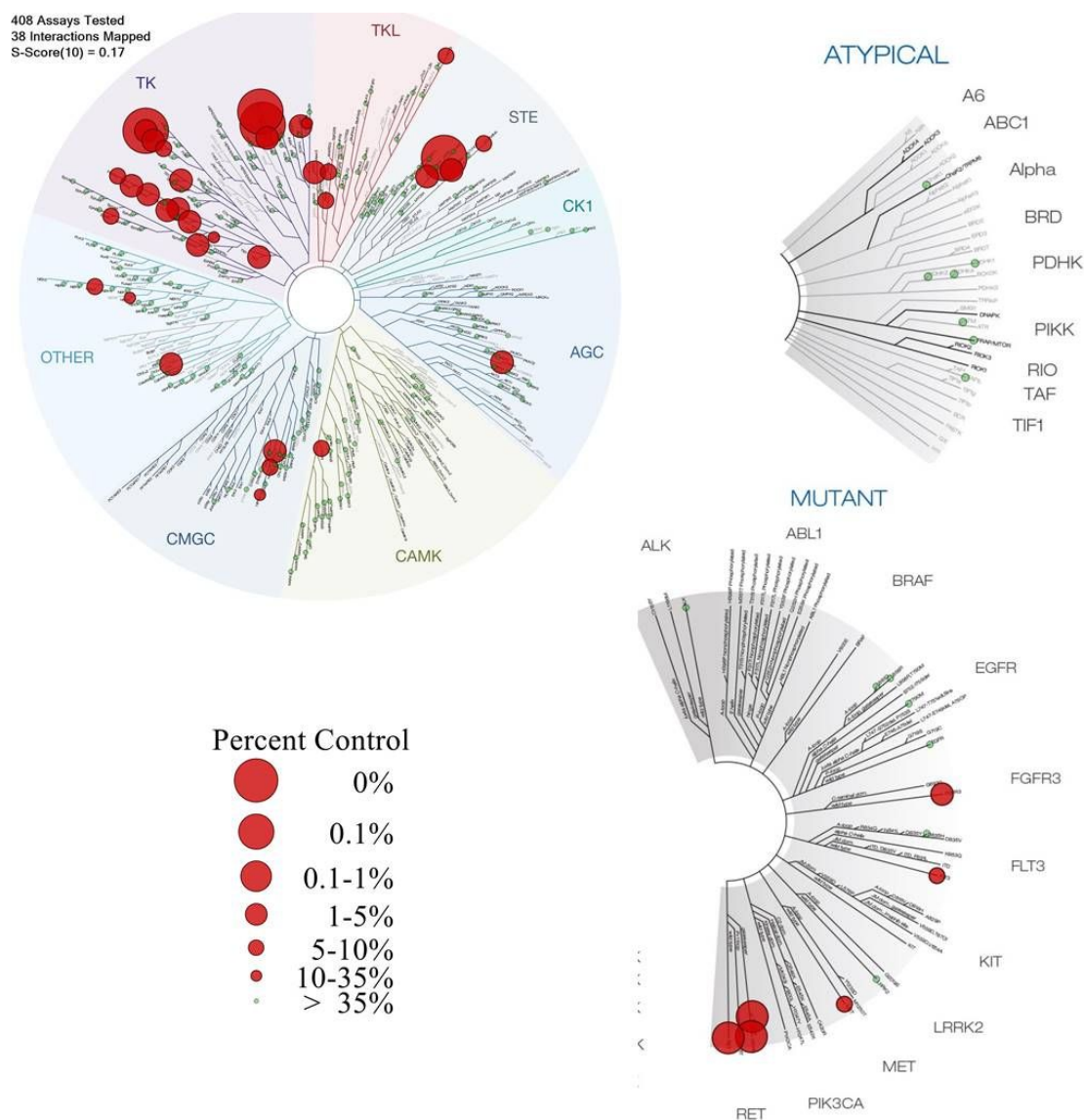


Figure 4. Wide kinome selectivity profiling of compound **9u** with Eurofins KinaseProfile platform. Tests were conducted at 0.1 μ M of compound **9u**. Treemap image was mapped by TREEspotTM software tool provided by DiscoverX corporation.

Clinically relevant FLT3-resitant mutants indicated poor prognosis and the dissociation constants (K_d) of **9u** against a panel of FLT3-ITD/TKD mutations were evaluated by DiscoverX Kinomescan technology. As displayed in Table 5, **9u** binds with high affinity to wt FLT3 and FLT3 mutants. In particular, **9u** displayed nice

binding affinity with drug-resistance mutants such as D835 mutants. As for the secondary ITD-TKD mutants, **9u** also showed considerable binding affinity for FLT3-ITD-D835V and FLT3-ITD-F691L mutants (K_d : 41.26 nM, 48.47 nM, respectively). The high affinity for those mutants conferring dramatical resistance to FLT3 inhibitory monotherapy made **9u** very promising for clinical applications.

Table 5. Dissociation Constants of Compound **9u** against Wt and Mutant FLT3 Kinases^a

Mutant type	K_d , nM
FLT3 wt	4.37
FLT3(D835V)	7.04
FLT3(ITD)	20.52
FLT3(ITD, D835V)	41.26
FLT3(ITD, F691L)	48.47
FLT3(N841I)	2.37
FLT3(R834Q)	10.15
FLT3(D835H)	5.14
FLT3(D835Y)	7.78
FLT3(K663Q)	2.48

^a The biochemical tests were provided by DiscoverX. All the data were obtained by duplicated test.

Molecular Docking of Compounds into FLT3 kinase. In order to further understand the different activities of compounds **9b**, **9u**, and **13a** against FLT3 kinase, we performed the molecular docking into FLT3. The active pocket of FLT3 kinase is narrow and long with a small opening at the bottom of the pocket to be communicated with the outside (PDB code 4XUF). Docking of **9b** into the FLT3 kinase (DFG-out

inactive conformation) indicated that compound **9b** was well embedded in the pocket, and the nitrogen atom of pyrimidine formed hydrogen bond with Cys694 residue (Figure 5C). Amino of pyrimidine formed one hydrogen bond with carbonyl of Glu692 residue. Additionally, the π - π stacking was formed between the linking phenyl with Phe691 and Phe830 residues. Canonical hydrogen bonds were formed between Glu661 and Asp829 by urea linkage. The hydrophobic pocket was occupied by the tert-butyl substituted isoxazole. Through these actions, **9b** occupied the active pocket well and restricted conformational changes of the FLT3 active pocket, thereby inhibiting FLT3 kinase activity. The docking pattern of compound **9u** was highly similar to **9b**, with one hydrogen bond loss between N at pyrimidine with Cys694, which led to slight decline of inhibitory activities against FLT3 and tumor cells (Figure 5A and 5B). However, the introduction of F atom to benzene ring (**13a**) blocked the hydrogen bond action between N-H of urea linkage and Glu661, which caused slight efficacy decrease in comparison to **9b** (Figure 5D).

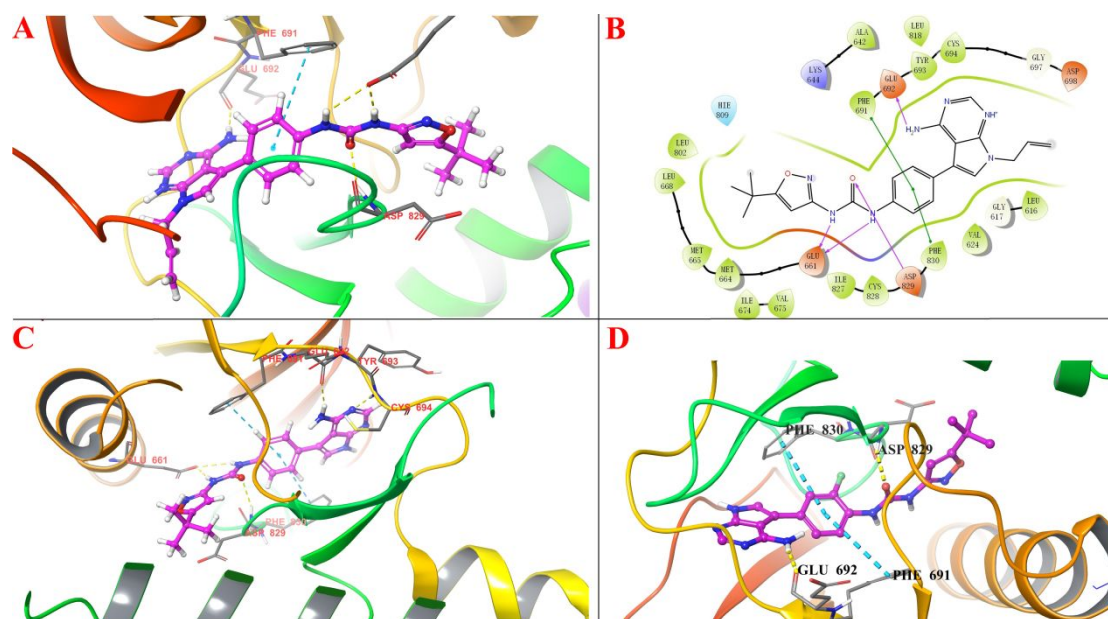


Figure 5. (A, B): Mimetic binding mode of compound **9u** (purple stick) within FLT3

protein; (C): Mimetic binding mode of compound **9b** (purple stick) within FLT3 protein; (D): Mimetic binding mode of compound **13a** (purple stick) within FLT3 protein. For clarity, nitrogen, oxygen and fluorine atoms are displayed in blue, red, and green, respectively.

Cell Cycle Arrest Assays and Apoptosis Assays by Flow Cytometry. MAPK and STAT pathways are crucial regulators of cell proliferation and their inhibition induce cell cycle arrest in the G₁/G₀ phase⁴⁵. Cell cycle analyses in MV4-11 and Molm-13 cells treated with compound **9u** were conducted. As shown in Figure 6A, **9u** strongly induced cell cycle arrest with G₁/G₀ percentage of 53% even at 1 nM compared to vehicle in Molm-13 cell. The percentage of G₁/G₀ cells populations increased from 53% to 94% after treatment with **9u** at 1 nM, 3 nM, and 10 nM. As expected, similar results were observed at the same concentration in MV4-11 cells. We next conducted apoptosis assays to confirm that compound **9u** could induce cell death. As exhibited in Figure 6C, the total apoptosis accounted for 34% when Molm-13 cells were treated with **9u** at 10 nM. Moreover, the apoptosis effects were strengthening as the dose increased. As expected, similar results were observed at the same concentration in MV4-11 cells. Obviously, compound **9u** blocked the AML cells in G₁ stage, which led to decreased S-phase and G₂-phase percentage and also induced AML cells apoptosis.

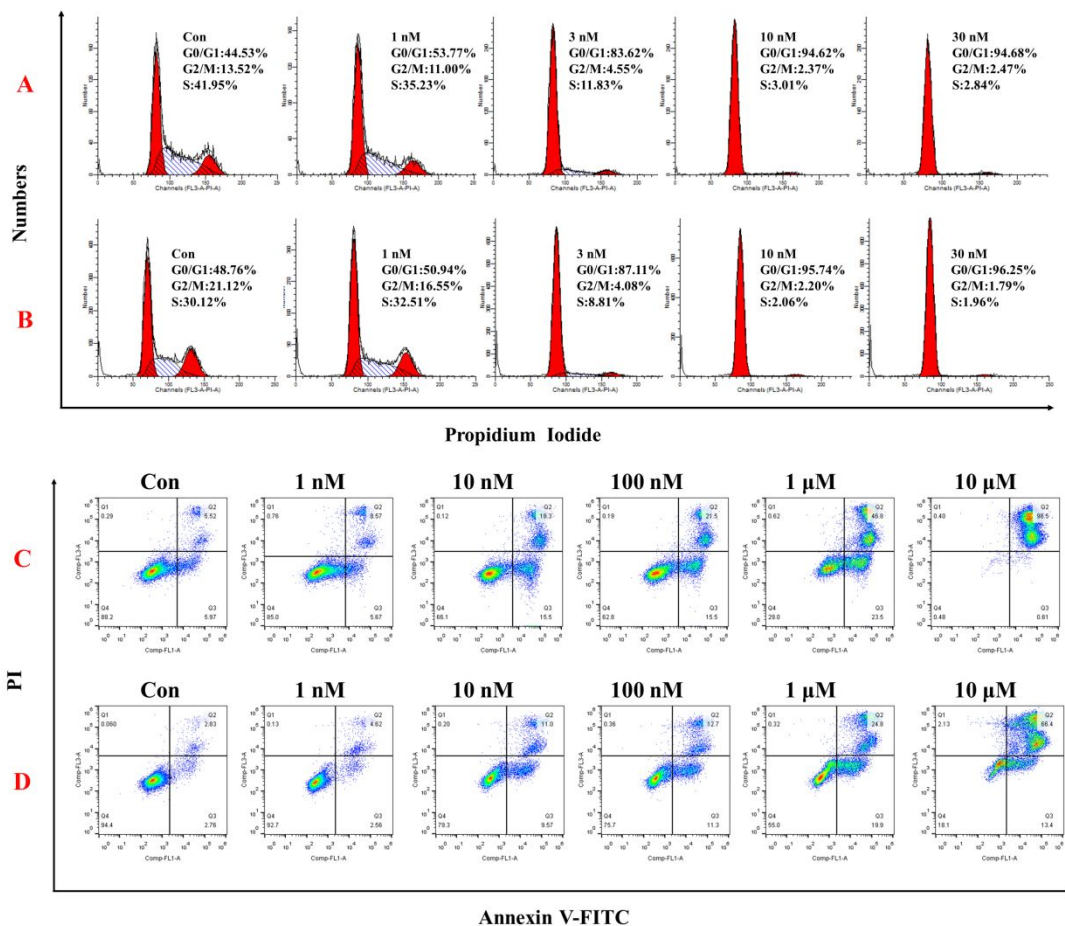


Figure 6. (A, B): Molm-13 and MV4-11 cells were incubated with compound **9u**, respectively. (C, D): Molm-13 and MV4-11 cells were incubated with compound **9u**, respectively.

Western Blot of Signaling Pathways for FLT3 Kinase. To further investigate whether the anti-tumor activities were relevant to inhibition of FLT3 and its downstream signal factors, we then examined the signaling proteins in Molm-13 and MV4-11 cells treated with compound **9u** by western blot and conducted densitometric quantification by ImageJ software. As the results showed (Figure 7), compound **9u** blocked FLT3 autophosphorylation at Tyr591 at 10 nM completely, which exhibited comparable inhibition effects with quizartinib. Notably, **9u** at 3 nM abolished phosphorylation of STAT5 at Y694, which was a direct substrate of the oncogenic

FLT3-ITD variant. Phosphorylation ERK at T202/Y204, one key component of MAPK signaling pathway, was obviously reduced upon treatment with compound **9u**. Similar results were obtained in MV4-11 cells when treated with compound **9u** (Figure 7).

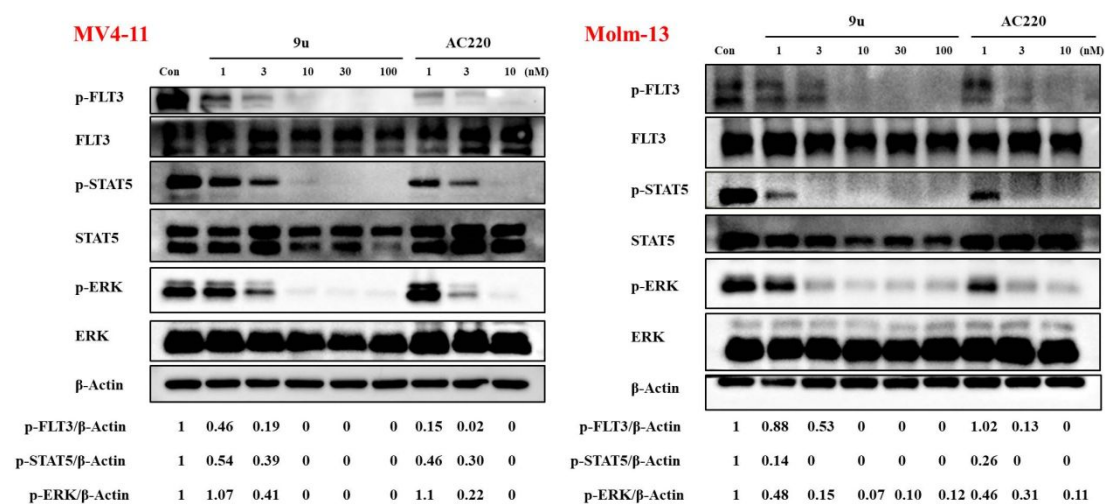


Figure 7. Compound **9u** inhibited phosphorylation of FLT3 and downstream signaling proteins STAT5 and ERK after treatment for 2 h.

Anti-tumor Efficacy in AML Xenograft Models. We then evaluated the anti-tumor efficacy of compound **9u** in Molm-13 and MV4-11 cells inoculated xenograft mouse models (Table 7). As shown in Figure 8A and 8B, **9u** significantly and dose-dependent inhibited the tumor growth both in Molm-13 and MV4-11 cells inoculated xenograft models. Oral administration of **9u** at 1 mg/kg showed potent antitumor effect and tumor growth inhibitory rate (TGI) was 77.9% in Molm-13 bearing mice model. Moreover, **9u** exhibited comparable antitumor activity with quizartinib (AC220) at dosage of 3 mg/kg. No obvious toxicity was observed during the treatment stage in all the experiment groups. Not surprisingly, **9u** also showed excellent anti-tumor activities in MV4-11 xenograft model (Table 6 and Figure 8B).

Treatment with **9u** at 3 mg/kg achieved one-third tumor regression on day 10. Both **9u** and quizartinib treatment groups achieved rapid and complete tumor extinction on day 8. Mice from control, 1 mg/kg, and 3 mg/kg groups were sacrificed on day 14 and tumors were extracted out and photographed subsequently. **9u** and quizartinib at 10 mg/kg groups continued to investigate the recurrence of tumor. After continuous treatment for prolonged 4 days, both **9u** and quizartinib groups were stopped treatment on day 18. However, two groups both recurred quickly at day 24 and 26, respectively. These results suggested that leukemic stem cells may lead to tumor recurrence due to the complex regulatory mechanisms, such as incomplete and discontinuous inhibition of FLT3^{17, 46}. We next determined to evaluate higher dosage for delaying or preventing tumor recurrence.

Table 6. Tumor Growth Inhibition of **9u** in Vivo.

Tumor models	Cmpd	Treatment			Survivors (day)	Tumor mass change(%)
		Schedule ^a	Dosage (mg/kg)	Route		
Molm-13	9u	QD×10	1	po	6/6	77.9
	9u	QD×10	3	po	6/6	94.5
	9u	QD×10	10	po	6/6	96.0
	quizartinib	QD×10	3	po	6/6	98.2
MV4-11	9u	QD×14	1	po	6/6	70.5
	9u	QD×14	3	po	6/6	98.2
	9u	QD×18	10	po	6/6	100
	quizartinib	QD×18	3	po	6/6	100

^a QD, per day.

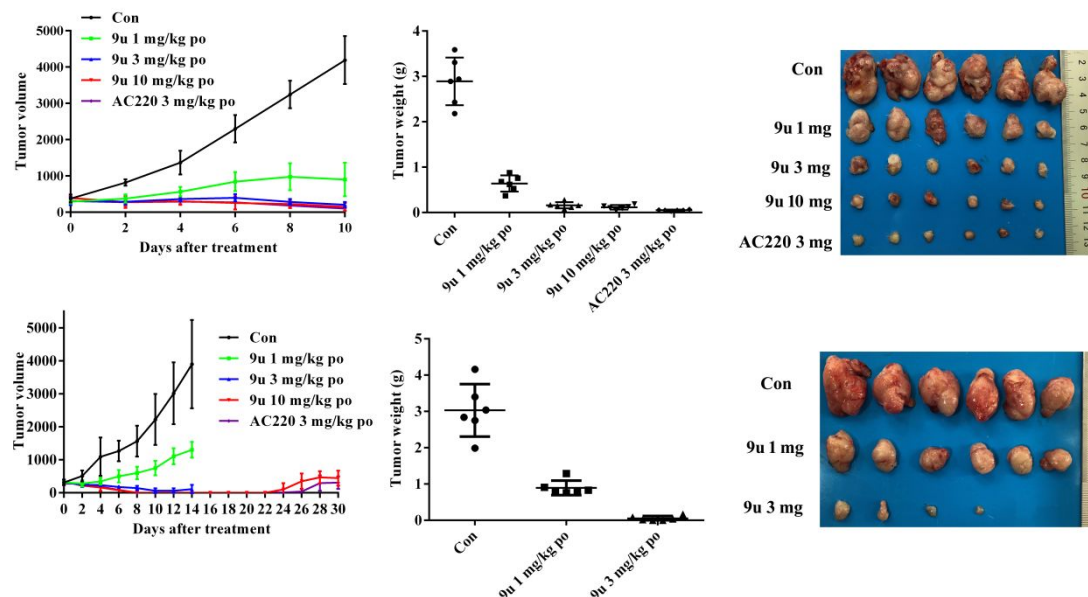


Figure 8. Anti-tumor activities of **9u** in Molm-13 and MV4-11 xenograft models.

Conclusion

FLT3-ITD/TKD resistant mutants conferred poor prognosis and higher relapsed rate after treatment with FLT3 inhibitors. Overcoming FLT3 mutants made it a promising drug design strategy for treating AML. Combination of advantages and disadvantages of clinical trials and applications of FLT3 inhibitors, we designed and synthesized a series of novel FLT3 kinase inhibitors. Compound **9u** possessed low nanomolar FLT3 kinase inhibitory activities and lower-dose anti-AML activities. It showed relatively good kinases selectivity and high binding affinity to FLT3 mutants. Compound **9u** also showed potent antiproliferation activities against MV4-11 and Molm-13 cells. It also showed excellent potent antiproliferation activities against FLT3-ITD-D835V and F691L cells which were resistant to quizartinib. Furthermore, **9u** had higher selectivity toward FLT3 relative to c-Kit than quizartinib, which might lower myelosuppression toxicity. Cellular assays demonstrated that **9u** inhibited phosphorylated FLT3 and downstream signaling factors and also induced cell cycle

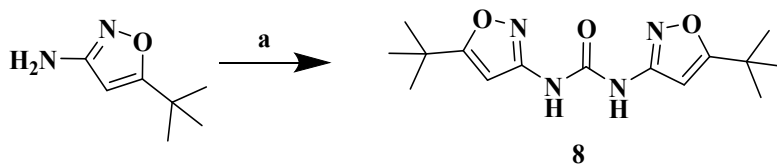
1
2
3
4 arrest in G₀/G₁ stage and apoptosis in MV4-11 and Molm-13 cells. Compound **9u**,
5
6 with high bioavailability, strongly suppressed tumor growth in Molm-13 model and
7
8
9 achieved rapid tumor regression at 10 mg/kg in MV4-11 model via oral
10
11
12 administration. All the reported results suggested that **9u** may be a potent candidate
13
14 for treating AML.
15
16
17
18
19
20
21
22
23
24
25
26
27
28
29
30
31
32
33
34
35
36
37
38
39
40
41
42
43
44
45
46
47
48
49
50
51
52
53
54
55
56
57
58
59
60

Experimental Section

Chemistry. All the chemical solvents and reagents, which were analytically pure without further purification, were commercially available. TLC was performed on 0.20 mm Silica Gel 60 F₂₅₄ plates (Qingdao Haiyang Chemical, China). ¹H NMR and ¹³C NMR spectra were recorded on Bruker Avance 400 spectrometer (Bruker Company, Germany), using TMS as an internal standard. Chemical shifts were given in ppm (parts per million). Mass spectra were recorded on Q-TOF Premier mass spectrometer (Micromass, Manchester, UK). The purity of each compound (> 95%) was determined on an Waters e2695 series LC system (column, Xtimate C18, 4.6 mm ×150 mm, 5 μm; mobile phase, methanol (70%)/H₂O (30%); low rate, 1.0 mL/min; UV wavelength, 254 - 400 nm; temperature, 25 °C; injection volume, 10 μL).

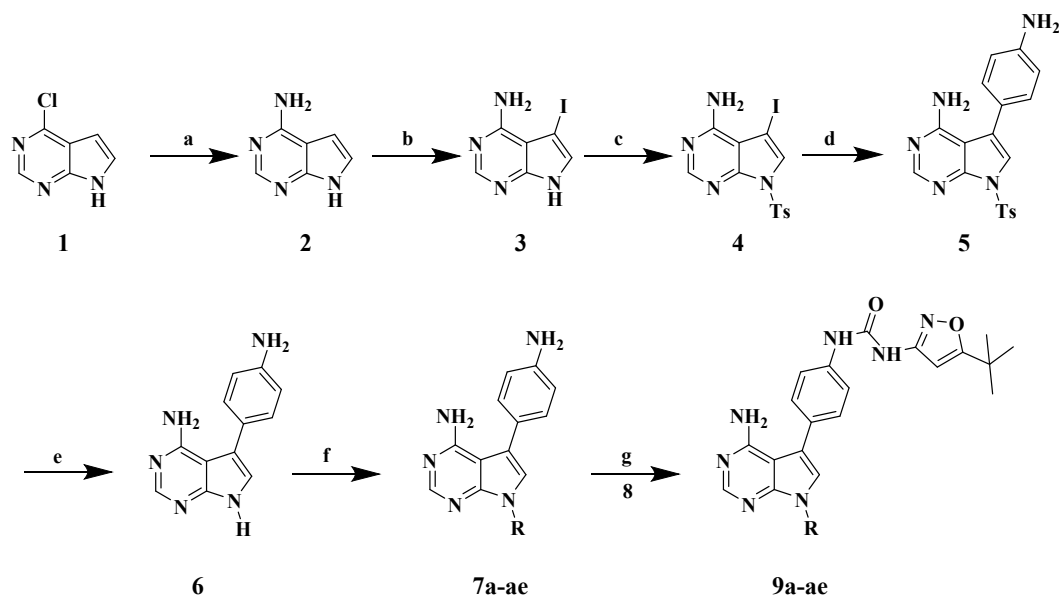
The general procedure to prepare compounds **9a-ae** has been shown in Scheme 1 and 2. 4-chloro-7*H*-pyrrolo[2,3-*d*]pyrimidine (**1**) was aminated with ammonium hydroxide to obtain **2**. Iodine was added to C-5 position of compound **2** by NIS to obtain **3**. Then N-H of **3** was protected by Ts group to give **4**. By Suzuki coupling reaction with 4-aminophenylboronic acid, **4** was converted to **5**. Under strong alkali condition, Ts group was removed from **5** to give **6**. 3-amino-5-tert-butylisoxazole was acylated by triphosgene with itself to give the key intermediate **8**. N-H of compound **6** was substituted by appropriate halide to give **7a-ae**. Then via ammonolysis **7a-ae** were converted to target molecules **9a-ae**.

Scheme 1. Synthesis of Intermediate **8^a**



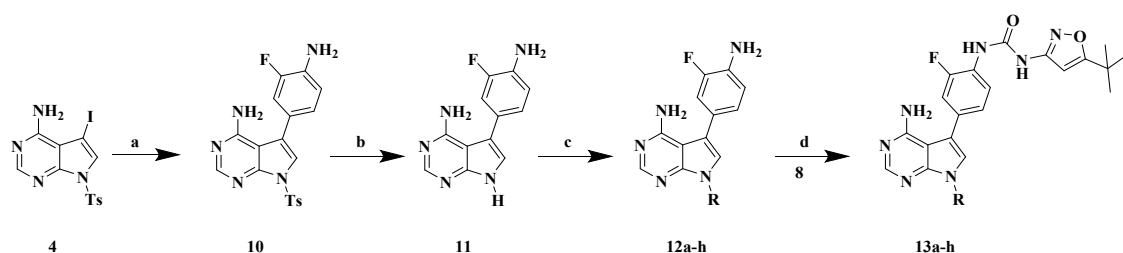
^a Reagent and condition: (a) Triphosgene, NEt₃, THF, 65 °C, 5 h.

Scheme 2. Syntheses of Compounds **9a-ae**^a



^a Reagents and conditions: (a) NH₃·H₂O, high pressure, 130 °C, 4 h; (b) NIS, THF, rt, 1 h; (c) TsCl, DMAP, NEt₃, CH₃CN, 80 °C, 2 h; (d) 4-aminophenylboronic acid, (dppf)PdCl₂, K₂CO₃, dioxane/EtOH/H₂O = 7/3/4(v/v/v), 80 °C, 2 h; (e) KOH, H₂O, rt, 1 h; (f) Appropriate halide, Cs₂CO₃, 80 °C, 1 h; (g) Intermediate **8**, CH₃CN, 80 °C, 1 h.

Scheme 3. Syntheses of Compounds **13a-h**^a



^a Reagents and conditions: (a) 4-amino-3-fluorobenzeneboronic acid pinacol ester,

(dppf)PdCl₂, K₂CO₃, dioxane/EtOH/H₂O = 7/3/4(v/v/v), 80 °C, 2 h; (b) KOH, H₂O, rt, 1 h; (c) Appropriate halide, Cs₂CO₃, 80 °C, 1 h; (d) Intermediate **8**, CH₃CN, 80 °C, 1 h.

General Procedures of Method A for the Syntheses of Compounds 9a-ae

7H-pyrrolo[2,3-*d*]pyrimidin-4-amine (2). Commercially available **1** (20 g, 50 mmol, 1 equiv) was added to ammonia solution (150 ml, 25-28% NH₃ in water) and the mixture reacted in high-pressure autoclave. After reaction for 4 h at 130 °C, the mixture was cooled to room temperature (rt). After filtration, the residue was washed with diethyl ether and dried at 80 °C for 2 h. The crude wasn't purified further. ¹H NMR (400 MHz, DMSO-*d*₆) δ: 11.45 (s, 1H), 8.03 (s, 1H), 7.06 (d, *J* = 3.2 Hz, 1H), 6.88 (s, 2H), 6.51 (d, *J* = 3.3 Hz, 1H).

5-iodo-7H-pyrrolo[2,3-*d*]pyrimidin-4-amine (3). To a solution of **2** (16 g, 112 mmol, 1 equiv) in tetrahydrofuran (THF) (200 ml) was added *N*-iodosuccinimide (NIS) (37.8 g, 168 mmol, 1.5 equiv) by proportion. After 1 h, the solvent was removed under reduced pressure to get the residue. The residue was dispersed in water (300 mL) and Na₂S₂O₃ • 5H₂O (13.9 g, 56 mmol, 0.5 equiv) was added whereafter. After stirring for 0.5 h, the mixture was filtered. The residue was washed with diethyl ether and dried at 80 °C for 2 h. The crude wasn't purified further. ¹H NMR (400 MHz, DMSO-*d*₆) δ: 11.97 (s, 1H), 8.07 (s, 1H), 7.36 (s, 1H), 6.56 (s, 2H).

5-iodo-7-tosyl-7H-pyrrolo[2,3-*d*]pyrimidin-4-amine (4). To the mixture of **3** (26 g, 100 mmol, 1 equiv) in CH₃CN (500 ml) was added 4-dimethylaminopyridine (DMAP) (14.6 g, 120 mmol, 1.2 equiv) and triethylamine (NEt₃) (26 ml, 200 mmol, 2

equiv). *p*-Toluenesulfonyl chloride (TsCl) (28.6 g, 150 mmol, 1.5 equiv) was dissolved in CH₃CN (100 mL) and added to the mixture by proportion. After 2 h at 80 °C, the solvent was removed under reduced pressure to get the residue. The residue was dispersed in CH₃CN (300 mL) and stirred for 1 h. The residue was filtered and washed with diethyl ether and dried at 80 °C for 2 h. The crude wasn't purified further. ¹H NMR (400 MHz, DMSO-*d*₆) δ: 8.20 (s, 1H), 8.00 (d, *J* = 8.4 Hz, 2H), 7.82 (s, 1H), 7.45 (d, *J* = 8.2 Hz, 2H), 6.94 (s, 2H), 2.37 (s, 3H).

5-(4-aminophenyl)-7-tosyl-7H-pyrrolo[2,3-*d*]pyrimidin-4-amine (5). **4** (10.7 g, 25.8 mmol, 1 equiv) was dissolved in 1,4-dioxane/ethanol/water (v:v:v, 7:3:4, 200 ml) and treated with 4-aminophenylboronic acid (4.9 g, 28.4 mmol, 1.1 equiv), PdCl₂(dppf), and K₂CO₃ (7.1 g, 51.6 mmol, 2 equiv). The vial was sealed and heated with stirring at 80 °C for 2 h. The solvent was removed under reduced pressure to get the residue without purification.

5-(4-aminophenyl)-7H-pyrrolo[2,3-*d*]pyrimidin-4-amine (6). The crude production **5** was dissolved in water (100 mL) and KOH solid was added by proportion until pH was up to 14. After 1 h, the Ts group was removed completely. The mixture was quenched with water and extracted with CH₂Cl₂. The organic layer was separated and washed with saturated brine. After dried over Na₂SO₄, the solvent was removed under reduced pressure to afford the residue. The residue was dispersed in diethyl ether (50 mL) and stirred for 1 h. The residue was filtered and washed with diethyl ether to get **6** as gray solid. ¹H NMR (400 MHz, DMSO-*d*₆) δ: 11.57 (s, 1H), 8.07 (s, 1H), 7.12 (d, *J* = 8.3 Hz, 2H), 7.03 (s, 1H), 6.66 (d, *J* = 8.3 Hz, 2H), 5.94 (s, 2H), 5.16 (s, 2H).

To a mixture of **6** (225 mg, 1 mmol, 1 equiv) in CH₃CN was added Cs₂CO₃ (650 mg, 2 mmol, 2 equiv), followed by appropriate halide (1.2 mmol, 1.2 equiv). After reacting at 80 °C for 1 h, the mixture was filtered to remove salts and the filtrate was concentrated under reduced pressure to afford the crude **7a-ae** without purification.

1,3-bis(5-(tert-butyl)isoxazol-3-yl)urea (8). To a solution of triphosgene (47.07 g, 156.9 mmol, 1.1 equiv) in THF (500 ml) was added 3-amino-5-tert-butylisoxazole (20 g, 142.6 mmol, 1 equiv) by proportion. Then NEt₃ (39.8 mL, 285.3 mmol, 2 equiv) was added drop by drop. After reaction at 65 °C for 5 h, the mixture was filtered and the solvent was removed under reduced pressure to get the residue. The crude wasn't purified further as pale yellow powder. ¹H NMR (400 MHz, DMSO-*d*₆) δ: 6.71 (s, 1H), 6.35 (s, 1H), 4.90 (s, 2H), 1.36 (s, 9H), 1.35 (s, 9H). MS (ESI), *m/z*: 307.37 [M+H⁺].

To a solution of intermediate **7a-ae** (1 mmol, 1 equiv) in CH₃CN (20 mL) was added **8** (306 mg, 1 mmol, 1 equiv). After reaction at 80 °C for 1 h, a large amount of solid formed and the solid was obtained by filter and washed by diethyl ether. The corresponding crude **9a-ae** wasn't purified further as off-white or pale yellow powder.

1-(4-(4-amino-7-(2-morpholinoethyl)-7H-pyrrolo[2,3-*d*]pyrimidin-5-yl)phenyl)-3-(5-(tert-butyl)isoxazol-3-yl)urea (9a). ¹H NMR (400 MHz, DMSO-*d*₆) δ: 9.53 (s, 1H), 8.91 (s, 1H), 8.14 (s, 1H), 7.56 (d, *J* = 8.3 Hz, 2H), 7.40 (d, *J* = 8.2 Hz, 2H), 7.33 (s, 1H), 6.52 (s, 1H), 6.06 (s, 2H), 4.29 (t, *J* = 6.3 Hz, 2H), 3.54 (s, 4H), 2.71 (t, *J* = 6.4 Hz, 2H), 2.46 (s, 4H), 1.31 (s, 9H). ¹³C NMR (101 MHz, DMSO-*d*₆) δ: 180.67, 158.86, 157.71, 151.95, 151.84, 150.71, 138.09, 129.48, 129.32, 123.90, 119.49,

115.16, 100.36, 92.92, 66.66, 58.15, 53.65, 41.24, 32.95, 28.83. HRMS (ESI), m/z : 505.2672 $[M+H^+]$.

1-(4-(4-amino-7*H*-pyrrolo[2,3-*d*]pyrimidin-5-yl)phenyl)-3-(5-(tert-butyl)isoxazol-3-yl)urea (9b). ^1H NMR (400 MHz, DMSO- d_6) δ : 11.74 (s, 1H), 9.53 (s, 1H), 8.93 (s, 1H), 8.11 (s, 1H), 7.55 (d, $J = 8.5$ Hz, 2H), 7.40 (d, $J = 8.5$ Hz, 2H), 7.19 (d, $J = 2.3$ Hz, 1H), 6.52 (s, 1H), 5.99 (s, 2H), 1.31 (s, 9H). ^{13}C NMR (101 MHz, DMSO- d_6) δ : 180.65, 158.86, 157.59, 152.01, 151.88, 151.79, 138.09, 129.78, 129.44, 120.45, 119.40, 115.90, 100.36, 92.94, 32.94, 28.83. HRMS (ESI), m/z : 392.1831 $[M+H^+]$.

tert-butyl-4-amino-5-(4-(3-(5-(tert-butyl)isoxazol-3-yl)ureido)phenyl)-7*H*-pyrrolo[2,3-*d*]pyrimidine-7-carboxylate (9c). ^1H NMR (400 MHz, DMSO- d_6) δ : 9.57 (s, 1H), 9.02 (s, 1H), 8.28 (s, 1H), 7.59 (d, $J = 8.6$ Hz, 2H), 7.47 (s, 1H), 7.44 (d, $J = 8.5$ Hz, 2H), 6.52 (s, 1H), 6.23 (s, 2H), 1.61 (s, 9H), 1.31 (s, 9H). HRMS (ESI), m/z : 592.2353 $[M+H^+]$.

tert-butyl-4-(2-(4-amino-5-(4-(3-(5-(tert-butyl)isoxazol-3-yl)ureido)phenyl)-7*H*-pyrrolo[2,3-*d*]pyrimidin-7-yl)ethyl)piperazine-1-carboxylate (9d). ^1H NMR (400 MHz, DMSO- d_6) δ : 9.53 (s, 1H), 8.91 (s, 1H), 8.14 (s, 1H), 7.56 (d, $J = 8.5$ Hz, 2H), 7.39 (d, $J = 8.5$ Hz, 2H), 7.33 (s, 1H), 6.52 (s, 1H), 6.06 (s, 2H), 4.29 (t, $J = 6.5$ Hz, 2H), 3.28 (s, 4H), 2.73 (t, $J = 6.5$ Hz, 2H), 2.46 – 2.37 (m, 4H), 1.39 (s, 9H), 1.31 (s, 9H). ^{13}C NMR (101 MHz, DMSO- d_6) δ : 180.67, 158.87, 157.70, 154.30, 151.95, 151.83, 150.70, 138.09, 129.47, 129.33, 123.89, 119.48, 115.17, 100.37, 92.92, 79.20, 57.66, 52.84, 41.47, 32.95, 28.83, 28.52. HRMS (ESI), m/z : 604.3353 $[M+H^+]$.

1-(4-(4-amino-7-(2-(piperazin-1-yl)ethyl)-7*H*-pyrrolo[2,3-*d*]pyrimidin-5-yl)phenyl

1-3-(5-(tert-butyl)isoxazol-3-yl)urea (9e). ^1H NMR (400 MHz, $\text{DMSO}-d_6$) δ : 9.58 (s, 1H), 9.01 (s, 1H), 8.14 (s, 1H), 7.57 (d, $J = 8.5$ Hz, 2H), 7.39 (d, $J = 8.5$ Hz, 2H), 7.33 (s, 1H), 6.52 (s, 1H), 6.05 (s, 2H), 4.27 (t, $J = 6.6$ Hz, 2H), 2.75 – 2.63 (m, 6H), 2.41 (s, 4H), 1.31 (s, 9H). ^{13}C NMR (101 MHz, $\text{DMSO}-d_6$) δ : 180.62, 158.86, 157.70, 151.92, 150.69, 138.20, 129.39, 129.30, 123.90, 119.41, 115.16, 100.36, 92.94, 58.14, 53.12, 45.28, 41.38, 32.94, 28.84. HRMS (ESI), m/z : 504.2829 $[\text{M}+\text{H}^+]$.

1-(4-(4-amino-7-(3-morpholinopropyl)-7H-pyrrolo[2,3-*d*]pyrimidin-5-yl)phenyl)-3-(5-(tert-butyl)isoxazol-3-yl)urea (9f). ^1H NMR (400 MHz, $\text{DMSO}-d_6$) δ : 9.53 (s, 1H), 8.90 (s, 1H), 8.14 (s, 1H), 7.56 (d, $J = 8.6$ Hz, 2H), 7.40 (d, $J = 8.6$ Hz, 2H), 7.31 (s, 1H), 6.52 (s, 1H), 6.05 (s, 2H), 4.20 (t, $J = 7.0$ Hz, 2H), 3.59 – 3.51 (m, 4H), 2.29 (dd, $J = 14.3, 7.0$ Hz, 6H), 2.02 – 1.91 (m, 2H), 1.31 (s, 9H). ^{13}C NMR (101 MHz, $\text{DMSO}-d_6$) δ : 180.68, 158.86, 157.71, 151.96, 151.83, 150.66, 138.07, 129.50, 129.34, 123.68, 119.48, 115.18, 100.45, 92.92, 66.65, 55.80, 53.71, 42.57, 32.95, 28.83, 27.07. HRMS (ESI), m/z : 519.2825 $[\text{M}+\text{H}^+]$.

1-(4-(4-amino-7-(2-(dimethylamino)ethyl)-7H-pyrrolo[2,3-*d*]pyrimidin-5-yl)phenyl)-3-(5-(tert-butyl)isoxazol-3-yl)urea (9g). ^1H NMR (400 MHz, $\text{DMSO}-d_6$) δ : 9.54 (s, 1H), 8.93 (s, 1H), 8.14 (s, 1H), 7.56 (d, $J = 8.3$ Hz, 2H), 7.39 (d, $J = 8.3$ Hz, 2H), 7.33 (s, 1H), 6.52 (s, 1H), 6.05 (s, 2H), 4.26 (t, $J = 6.6$ Hz, 2H), 2.67 (t, $J = 6.5$ Hz, 2H), 2.20 (s, 6H), 1.31 (s, 9H). ^{13}C NMR (101 MHz, $\text{DMSO}-d_6$) δ : 180.65, 158.87, 157.70, 151.93, 151.85, 150.71, 138.11, 129.47, 129.31, 123.73, 119.46, 115.17, 100.36, 92.93, 58.93, 45.57, 42.00, 32.94, 28.83. HRMS (ESI), m/z : 463.2563 $[\text{M}+\text{H}^+]$.

1-(4-(4-amino-7-methyl-7H-pyrrolo[2,3-d]pyrimidin-5-yl)phenyl)-3-(5-(tert-butyl)isoxazol-3-yl)urea (9h). ¹H NMR (400 MHz, DMSO-*d*₆) δ : 9.79 (s, 1H), 9.57 (s, 1H), 8.49 (s, 1H), 7.62 (s, 1H), 7.41 (d, *J* = 8.6 Hz, 2H), 7.11 (d, *J* = 8.5 Hz, 2H), 6.53 (s, 1H), 3.85 (s, 3H), 1.31 (s, 9H). ¹³C NMR (101 MHz, DMSO-*d*₆) δ : 180.56, 158.74, 152.05, 151.72, 147.94, 142.85, 139.28, 129.35, 127.76, 126.63, 119.29, 118.32, 98.85, 92.97, 32.93, 32.06, 28.85. HRMS (ESI), *m/z*: 406.1992 [M+H⁺].

1-(4-(4-amino-7-ethyl-7H-pyrrolo[2,3-d]pyrimidin-5-yl)phenyl)-3-(5-(tert-butyl)isoxazol-3-yl)urea (9i). ¹H NMR (400 MHz, DMSO-*d*₆) δ : 9.78 (s, 1H), 9.61 (s, 1H), 8.48 (s, 1H), 7.69 (s, 1H), 7.61 (d, *J* = 8.6 Hz, 2H), 7.42 (d, *J* = 8.5 Hz, 2H), 6.53 (s, 1H), 4.30 (q, *J* = 7.2 Hz, 2H), 1.43 (t, *J* = 7.2 Hz, 3H), 1.31 (s, 9H). ¹³C NMR (101 MHz, DMSO-*d*₆) δ : 180.52, 158.74, 152.08, 151.82, 147.40, 142.80, 139.30, 129.36, 126.68, 126.30, 119.22, 118.52, 98.91, 92.97, 32.93, 28.85, 15.84. HRMS (ESI), *m/z*: 420.2142 [M+H⁺].

1-(4-(4-amino-7-isopropyl-7H-pyrrolo[2,3-d]pyrimidin-5-yl)phenyl)-3-(5-(tert-butyl)isoxazol-3-yl)urea (9j). ¹H NMR (400 MHz, DMSO-*d*₆) δ : 9.55 (s, 1H), 8.97 (s, 1H), 8.33 (s, 1H), 7.65 (s, 1H), 7.59 (d, *J* = 8.6 Hz, 2H), 7.43 (d, *J* = 8.5 Hz, 2H), 6.52 (s, 1H), 5.10 – 4.93 (m, 1H), 1.49 (d, *J* = 6.8 Hz, 6H), 1.31 (s, 9H). ¹³C NMR (101 MHz, DMSO-*d*₆) δ : 180.71, 171.97, 158.82, 153.98, 151.81, 148.27, 146.51, 138.59, 129.46, 128.10, 122.43, 119.47, 117.44, 99.57, 92.92, 32.95, 28.83, 22.97, 22.76. HRMS (ESI), *m/z*: 434.2299 [M+H⁺].

1-(4-(4-amino-7-propyl-7H-pyrrolo[2,3-d]pyrimidin-5-yl)phenyl)-3-(5-(tert-butyl)isoxazol-3-yl)urea (9k). ¹H NMR (400 MHz, DMSO-*d*₆) δ : 9.80 (s, 1H), 9.66 (s,

1H), 8.48 (s, 1H), 7.68 (s, 1H), 7.61 (d, $J = 8.5$ Hz, 2H), 7.41 (d, $J = 8.5$ Hz, 2H), 6.53 (s, 1H), 4.23 (t, $J = 7.0$ Hz, 2H), 1.90 – 1.77 (m, 2H), 1.31 (s, 9H), 0.87 (t, $J = 7.4$ Hz, 3H). ^{13}C NMR (101 MHz, DMSO- d_6) δ : 180.55, 158.75, 152.04, 151.80, 147.79, 142.88, 139.27, 129.40, 126.76, 126.69, 119.27, 118.44, 98.84, 92.97, 46.64, 32.93, 28.85, 23.50, 11.44. HRMS (ESI), m/z : 434.2303 [$\text{M}+\text{H}^+$].

1-(4-(4-amino-7-butyl-7H-pyrrolo[2,3-d]pyrimidin-5-yl)phenyl)-3-(5-(tert-butyl)isoxazol-3-yl)urea (9l). ^1H NMR (400 MHz, DMSO- d_6) δ : 9.78 (s, 1H), 9.61 (s, 1H), 8.48 (s, 1H), 7.68 (s, 1H), 7.61 (d, $J = 8.6$ Hz, 2H), 7.41 (d, $J = 8.5$ Hz, 2H), 6.53 (s, 1H), 4.26 (t, $J = 7.1$ Hz, 2H), 1.87 – 1.75 (m, 2H), 1.31 (s, 9H), 1.26 (dd, $J = 14.9, 7.5$ Hz, 2H), 0.91 (t, $J = 7.4$ Hz, 3H). ^{13}C NMR (101 MHz, DMSO- d_6) δ : 180.55, 158.75, 152.02, 151.68, 147.70, 142.76, 139.26, 129.39, 126.76, 126.66, 119.28, 118.53, 98.80, 92.96, 44.78, 32.92, 32.13, 28.84, 19.75, 13.88. HRMS (ESI), m/z : 448.2460 [$\text{M}+\text{H}^+$].

1-(4-(4-amino-7-hexyl-7H-pyrrolo[2,3-d]pyrimidin-5-yl)phenyl)-3-(5-(tert-butyl)isoxazol-3-yl)urea (9m). ^1H NMR (400 MHz, DMSO- d_6) δ : 9.71 (s, 1H), 9.40 (s, 1H), 8.46 (s, 1H), 7.67 (s, 1H), 7.61 (d, $J = 8.6$ Hz, 2H), 7.41 (d, $J = 8.5$ Hz, 2H), 6.52 (s, 1H), 4.25 (t, $J = 7.1$ Hz, 2H), 1.88 – 1.77 (m, 2H), 1.31 (s, 9H), 1.28 (m, 6H), 0.86 (t, $J = 6.8$ Hz, 3H). ^{13}C NMR (101 MHz, DMSO- d_6) δ : 180.54, 158.75, 152.02, 151.68, 147.69, 142.75, 139.27, 129.38, 126.75, 126.66, 119.28, 118.52, 98.79, 92.96, 45.06, 32.93, 31.13, 30.03, 28.84, 26.11, 22.38, 14.31. HRMS (ESI), m/z : 476.2770 [$\text{M}+\text{H}^+$].

1-(4-(4-amino-7-cyclopentyl-7H-pyrrolo[2,3-d]pyrimidin-5-yl)phenyl)-3-(5-(tert-butyl)isoxazol-3-yl)urea (9n). ^1H NMR (400 MHz, DMSO- d_6) δ : 9.78 (s, 1H), 9.62

(s, 1H), 8.47 (s, 1H), 7.73 (s, 1H), 7.61 (d, $J = 8.6$ Hz, 2H), 7.44 (d, $J = 8.5$ Hz, 2H), 6.53 (s, 1H), 5.22 – 5.08 (m, 1H), 2.16 (d, $J = 7.9$ Hz, 2H), 2.02 – 1.83 (m, 4H), 1.71 (d, $J = 7.0$ Hz, 2H), 1.31 (s, 9H). ^{13}C NMR (101 MHz, DMSO- d_6) δ : 180.51, 158.73, 152.08, 151.80, 147.66, 142.61, 139.32, 129.47, 126.69, 124.20, 119.15, 118.90, 99.03, 92.98, 56.11, 32.92, 32.79, 28.85, 24.21. HRMS (ESI), m/z : 460.2457 [$\text{M}+\text{H}^+$].

1-(4-(4-amino-7-benzyl-7H-pyrrolo[2,3-*d*]pyrimidin-5-yl)phenyl)-3-(5-(tert-butyl)isoxazol-3-yl)urea (9o). ^1H NMR (400 MHz, DMSO- d_6) δ : 9.71 (s, 1H), 8.49 (s, 1H), 7.74 (s, 1H), 7.60 (d, $J = 8.6$ Hz, 2H), 7.41 (d, $J = 8.5$ Hz, 2H), 7.38 – 7.27 (m, 5H), 6.52 (s, 1H), 5.49 (s, 2H), 1.31 (s, 9H). ^{13}C NMR (101 MHz, DMSO- d_6) δ : 180.59, 158.75, 151.98, 151.79, 147.78, 143.31, 139.29, 137.27, 129.42, 129.21, 128.36, 128.16, 126.70, 126.55, 119.31, 118.90, 99.09, 92.97, 48.46, 32.93, 28.84. HRMS (ESI), m/z : 482.2303 [$\text{M}+\text{H}^+$].

1-(4-(4-amino-7-(4-hydroxybutyl)-7H-pyrrolo[2,3-*d*]pyrimidin-5-yl)phenyl)-3-(5-(tert-butyl)isoxazol-3-yl)urea (9p). ^1H NMR (400 MHz, DMSO- d_6) δ : 9.53 (s, 1H), 8.91 (s, 1H), 8.14 (s, 1H), 7.56 (d, $J = 8.4$ Hz, 2H), 7.40 (d, $J = 8.4$ Hz, 2H), 7.32 (s, 1H), 6.52 (s, 1H), 6.05 (s, 2H), 4.41 (t, $J = 5.2$ Hz, 1H), 4.17 (t, $J = 7.0$ Hz, 2H), 4.09 (q, $J = 5.2$ Hz, 1H), 3.41 (dd, $J = 11.8, 6.2$ Hz, 2H), 3.18 (d, $J = 5.2$ Hz, 2H), 1.88 – 1.76 (m, 2H), 1.46 – 1.36 (m, 2H), 1.31 (s, 9H). ^{13}C NMR (101 MHz, DMSO- d_6) δ : 180.68, 158.86, 157.71, 151.95, 151.83, 150.64, 138.08, 129.48, 129.36, 123.53, 119.46, 115.23, 100.37, 92.93, 60.75, 44.09, 32.95, 30.16, 28.83, 27.05. HRMS (ESI), m/z : 464.2409 [$\text{M}+\text{H}^+$].

4-amino-5-(4-(3-(5-(tert-butyl)isoxazol-3-yl)ureido)phenyl)-N,N-diethyl-7H-pyrr

olo[2,3-*d*]pyrimidine-7-carboxamide (9q). ¹H NMR (400 MHz, DMSO-*d*₆) δ : 9.55 (s, 1H), 8.96 (s, 1H), 8.20 (s, 1H), 7.58 (d, *J* = 8.6 Hz, 2H), 7.44 (d, *J* = 8.5 Hz, 2H), 7.41 (s, 1H), 6.53 (s, 1H), 6.25 (s, 2H), 3.39 (m, 4H), 1.31 (s, 9H), 1.21 – 1.06 (m, 6H). ¹³C NMR (101 MHz, DMSO-*d*₆) δ : 180.69, 158.84, 158.04, 153.19, 151.83, 151.53, 150.56, 138.71, 129.57, 128.19, 121.42, 119.42, 117.82, 100.52, 92.93, 55.37, 32.95, 28.83. HRMS (ESI), *m/z*: 491.2493 [M+H⁺].

1-(4-(4-amino-7-(2-(4-(methylsulfonyl)piperazin-1-yl)ethyl)-7*H*-pyrrolo[2,3-*d*]pyrimidin-5-yl)phenyl)-3-(5-(tert-butyl)isoxazol-3-yl)urea (9r). ¹H NMR (400 MHz, DMSO-*d*₆) δ : 9.53 (s, 1H), 8.92 (s, 1H), 8.15 (s, 1H), 7.56 (d, *J* = 8.6 Hz, 2H), 7.40 (d, *J* = 8.5 Hz, 2H), 7.34 (s, 1H), 6.52 (s, 1H), 6.05 (s, 2H), 4.30 (t, *J* = 6.4 Hz, 2H), 3.12 – 3.03 (m, 4H), 2.85 (s, 3H), 2.79 (t, *J* = 6.5 Hz, 2H), 2.62 – 2.54 (m, 4H), 1.31 (s, 9H). HRMS (ESI), *m/z*: 582.2610 [M+H⁺].

1-(4-(4-amino-7-(2-methoxyethyl)-7*H*-pyrrolo[2,3-*d*]pyrimidin-5-yl)phenyl)-3-(5-(tert-butyl)isoxazol-3-yl)urea (9s). ¹H NMR (400 MHz, DMSO-*d*₆) δ : 9.56 (s, 1H), 8.95 (s, 1H), 8.15 (s, 1H), 7.56 (d, *J* = 8.4 Hz, 2H), 7.39 (d, *J* = 8.4 Hz, 2H), 7.29 (s, 1H), 6.53 (s, 1H), 6.09 (s, 2H), 4.33 (t, *J* = 5.3 Hz, 2H), 3.71 (t, *J* = 5.4 Hz, 2H), 3.26 (s, 3H), 1.31 (s, 9H). ¹³C NMR (101 MHz, DMSO-*d*₆) δ : 180.68, 158.86, 157.70, 151.95, 151.84, 150.74, 138.13, 129.37, 129.33, 123.87, 119.47, 115.23, 100.41, 92.93, 70.96, 58.40, 43.72, 32.95, 28.84. HRMS (ESI), *m/z*: 450.2249 [M+H⁺].

1-(4-(4-amino-7-(2-ethoxyethyl)-7*H*-pyrrolo[2,3-*d*]pyrimidin-5-yl)phenyl)-3-(5-(tert-butyl)isoxazol-3-yl)urea (9t). ¹H NMR (400 MHz, DMSO-*d*₆) δ : 9.53 (s, 1H), 8.92 (s, 1H), 8.15 (s, 1H), 7.56 (d, *J* = 8.4 Hz, 2H), 7.39 (d, *J* = 8.4 Hz, 2H), 7.29 (s,

1H), 6.52 (s, 1H), 6.06 (s, 2H), 4.32 (t, $J = 5.4$ Hz, 2H), 3.74 (t, $J = 5.5$ Hz, 2H), 3.46 (q, $J = 6.9$ Hz, 2H), 1.31 (s, 9H). ^{13}C NMR (101 MHz, $\text{DMSO-}d_6$) δ : 180.56, 158.75, 152.02, 151.77, 147.78, 142.95, 139.26, 135.00, 129.37, 126.69, 119.29, 118.38, 118.02, 98.85, 92.96, 44.33, 34.25, 32.93, 28.84. HRMS (ESI), m/z : 464.2406 $[\text{M}+\text{H}^+]$.

1-(4-(7-allyl-4-amino-7H-pyrrolo[2,3-d]pyrimidin-5-yl)phenyl)-3-(5-(tert-butyl)isoxazol-3-yl)urea (9u). ^1H NMR (400 MHz, $\text{DMSO-}d_6$) δ : 9.53 (s, 1H), 8.91 (s, 1H), 8.15 (s, 1H), 7.56 (d, $J = 8.5$ Hz, 2H), 7.40 (d, $J = 8.4$ Hz, 2H), 7.25 (s, 1H), 6.52 (s, 1H), 6.06 (m, 3H), 5.18 (d, $J = 10.1$ Hz, 1H), 5.09 (d, $J = 17.1$ Hz, 1H), 4.81 (d, $J = 5.4$ Hz, 2H), 1.31 (s, 9H). ^{13}C NMR (101 MHz, $\text{DMSO-}d_6$) δ : 180.64, 158.77, 152.59, 151.93, 148.08, 144.53, 139.08, 133.75, 129.43, 127.04, 126.11, 119.39, 118.36, 118.26, 99.20, 92.95, 47.13, 32.95, 28.84. HRMS (ESI), m/z : 432.2149 $[\text{M}+\text{H}^+]$.

1-(4-(4-amino-7-(but-3-en-1-yl)-7H-pyrrolo[2,3-d]pyrimidin-5-yl)phenyl)-3-(5-(tert-butyl)isoxazol-3-yl)urea (9v). ^1H NMR (400 MHz, $\text{DMSO-}d_6$) δ : 9.57 (s, 1H), 8.99 (s, 1H), 8.15 (s, 1H), 7.56 (d, $J = 8.4$ Hz, 2H), 7.39 (d, $J = 8.3$ Hz, 2H), 7.32 (s, 1H), 6.52 (s, 1H), 6.05 (s, 2H), 5.82 (ddd, $J = 23.8, 10.3, 6.7$ Hz, 1H), 5.14 – 4.93 (m, 2H), 4.24 (t, $J = 7.0$ Hz, 2H), 2.56 (dd, $J = 13.3, 6.5$ Hz, 2H), 1.31 (s, 9H). ^{13}C NMR (101 MHz, $\text{DMSO-}d_6$) δ : 180.67, 158.86, 157.71, 151.97, 151.85, 150.63, 138.13, 135.58, 129.43, 129.34, 123.50, 119.44, 117.54, 115.21, 100.41, 92.93, 43.48, 34.42, 32.95, 28.83. HRMS (ESI), m/z : 446.2302 $[\text{M}+\text{H}^+]$.

1-(4-(4-amino-7-(3-methylbut-2-en-1-yl)-7H-pyrrolo[2,3-d]pyrimidin-5-yl)phenyl)-3-(5-(tert-butyl)isoxazol-3-yl)urea (9w). ^1H NMR (400 MHz, $\text{DMSO-}d_6$) δ : 9.53

(s, 1H), 8.92 (s, 1H), 8.15 (s, 1H), 7.56 (d, $J = 8.4$ Hz, 2H), 7.39 (d, $J = 8.4$ Hz, 2H), 7.23 (s, 1H), 6.52 (s, 1H), 6.05 (s, 2H), 5.41 (t, $J = 6.8$ Hz, 1H), 4.76 (d, $J = 7.0$ Hz, 2H), 1.81 (s, 3H), 1.72 (s, 3H), 1.31 (s, 9H). ^{13}C NMR (101 MHz, DMSO- d_6) δ : 180.66, 158.86, 157.70, 152.04, 151.85, 150.32, 138.13, 136.47, 129.40, 129.35, 122.91, 120.60, 119.42, 115.49, 100.39, 92.93, 41.77, 32.95, 28.83, 25.81, 18.32. HRMS (ESI), m/z : 460.2457 [$\text{M}+\text{H}^+$].

1-(4-(4-amino-7-(2-methylallyl)-7H-pyrrolo[2,3-*d*]pyrimidin-5-yl)phenyl)-3-(5-(tert-butyl)isoxazol-3-yl)urea (9x). ^1H NMR (400 MHz, DMSO- d_6) δ : 9.53 (s, 1H), 8.92 (s, 1H), 8.15 (s, 1H), 7.56 (d, $J = 8.6$ Hz, 2H), 7.40 (d, $J = 8.6$ Hz, 2H), 7.20 (s, 1H), 6.52 (s, 1H), 6.09 (s, 2H), 4.87 (s, 1H), 4.73 (s, 2H), 4.61 (s, 1H), 1.68 (s, 3H), 1.31 (s, 9H). ^{13}C NMR (101 MHz, DMSO- d_6) δ : 180.66, 158.86, 157.78, 152.18, 151.83, 150.88, 142.16, 138.19, 129.39, 129.28, 123.45, 119.45, 115.69, 112.35, 100.25, 92.93, 49.50, 32.94, 28.82, 20.37. HRMS (ESI), m/z : 446.2298 [$\text{M}+\text{H}^+$].

1-(4-(4-amino-7-(pent-4-en-1-yl)-7H-pyrrolo[2,3-*d*]pyrimidin-5-yl)phenyl)-3-(5-(tert-butyl)isoxazol-3-yl)urea (9y). ^1H NMR (400 MHz, DMSO- d_6) δ : 9.77 (s, 1H), 9.58 (s, 1H), 8.48 (s, 1H), 7.68 (s, 1H), 7.61 (d, $J = 8.6$ Hz, 2H), 7.42 (d, $J = 8.6$ Hz, 2H), 6.53 (s, 1H), 5.83 (ddt, $J = 16.8, 10.2, 6.4$ Hz, 1H), 5.09 – 4.95 (m, 2H), 4.27 (t, $J = 7.0$ Hz, 2H), 2.05 (dd, $J = 13.7, 6.7$ Hz, 2H), 1.99 – 1.87 (m, 2H), 1.31 (s, 9H). ^{13}C NMR (101 MHz, DMSO- d_6) δ : 180.55, 158.75, 152.03, 151.74, 147.76, 142.84, 139.27, 137.85, 129.39, 126.73, 126.67, 119.28, 118.55, 115.96, 98.88, 92.96, 44.63, 32.93, 30.65, 29.20, 28.84. HRMS (ESI), m/z : 460.2458 [$\text{M}+\text{H}^+$].

1-(4-(4-amino-7-(hex-5-en-1-yl)-7H-pyrrolo[2,3-*d*]pyrimidin-5-yl)phenyl)-3-(5-(te

rt-butyl)isoxazol-3-yl)urea (9z). ¹H NMR (400 MHz, DMSO-*d*₆) δ : 9.78 (s, 1H), 9.60 (s, 1H), 8.48 (s, 1H), 7.68 (s, 1H), 7.61 (d, *J* = 8.6 Hz, 2H), 7.41 (d, *J* = 8.6 Hz, 2H), 6.53 (s, 1H), 5.78 (ddt, *J* = 16.9, 10.2, 6.7 Hz, 1H), 5.05 – 4.90 (m, 2H), 4.27 (t, *J* = 7.0 Hz, 2H), 2.06 (q, *J* = 7.2 Hz, 2H), 1.83 (dt, *J* = 14.9, 7.2 Hz, 2H), 1.41 – 1.31 (m, 2H), 1.31 (s, 9H). ¹³C NMR (101 MHz, DMSO-*d*₆) δ : 180.55, 158.75, 152.03, 151.76, 147.73, 142.86, 139.27, 138.75, 129.39, 126.72, 126.67, 119.27, 118.52, 115.55, 98.83, 92.96, 44.90, 33.03, 32.93, 29.58, 28.84, 25.73. HRMS (ESI), *m/z*: 474.2618 [M+H⁺].

1-(4-(4-amino-7-(prop-2-yn-1-yl)-7H-pyrrolo[2,3-*d*]pyrimidin-5-yl)phenyl)-3-(5-(tert-butyl)isoxazol-3-yl)urea (9aa). ¹H NMR (400 MHz, DMSO-*d*₆) δ : 9.66 (s, 1H), 9.28 (s, 1H), 8.49 (s, 1H), 7.66 (s, 1H), 7.61 (d, *J* = 8.5 Hz, 2H), 7.43 (d, *J* = 8.5 Hz, 2H), 6.52 (s, 1H), 5.15 (d, *J* = 2.3 Hz, 2H), 3.52 (t, *J* = 2.4 Hz, 2H), 1.31 (s, 9H). ¹³C NMR (101 MHz, DMSO-*d*₆) δ : 180.63, 158.75, 151.95, 151.84, 147.54, 143.60, 139.33, 129.45, 126.41, 125.92, 119.38, 119.06, 99.28, 92.96, 78.54, 76.82, 34.59, 32.94, 28.84. HRMS (ESI), *m/z*: 430.1985 [M+H⁺].

1-(4-(4-amino-7-(but-2-yn-1-yl)-7H-pyrrolo[2,3-*d*]pyrimidin-5-yl)phenyl)-3-(5-(tert-butyl)isoxazol-3-yl)urea (9ab). ¹H NMR (400 MHz, DMSO-*d*₆) δ : 9.55 (s, 1H), 8.97 (s, 1H), 8.17 (s, 1H), 7.57 (d, *J* = 8.5 Hz, 2H), 7.41 (d, *J* = 8.4 Hz, 2H), 7.32 (s, 1H), 6.53 (s, 1H), 6.12 (s, 1H), 4.97 (d, *J* = 2.3 Hz, 2H), 1.81 (dd, *J* = 5.3, 3.1 Hz, 3H), 1.31 (s, 9H). ¹³C NMR (101 MHz, DMSO-*d*₆) δ : 180.68, 158.86, 157.79, 152.28, 151.85, 150.27, 138.28, 129.38, 129.10, 122.67, 119.47, 115.99, 100.45, 92.93, 80.96, 74.98, 33.79, 32.95, 28.83, 3.54. HRMS (ESI), *m/z*: 444.2147 [M+H⁺].

1-(4-(4-amino-7-(pent-2-yn-1-yl)-7H-pyrrolo[2,3-d]pyrimidin-5-yl)phenyl)-3-(5-(tert-butyl)isoxazol-3-yl)urea (9ac). ¹H NMR (400 MHz, DMSO-*d*₆) δ : 9.53 (s, 1H), 8.93 (s, 1H), 8.16 (s, 1H), 7.56 (d, *J* = 8.6 Hz, 2H), 7.40 (d, *J* = 8.5 Hz, 2H), 7.31 (s, 1H), 6.52 (s, 1H), 6.12 (s, 2H), 4.98 (t, *J* = 2.1 Hz, 2H), 2.25 – 2.16 (m, 2H), 1.30 (s, 9H), 1.06 (t, *J* = 7.5 Hz, 3H). ¹³C NMR (101 MHz, DMSO-*d*₆) δ : 180.68, 158.86, 157.79, 152.28, 151.84, 150.27, 138.28, 129.38, 129.10, 122.58, 119.49, 116.00, 100.44, 92.93, 86.47, 75.10, 33.76, 32.95, 28.83, 14.02, 12.10. HRMS (ESI), *m/z*: 458.2299 [M+H⁺].

1-(4-(4-amino-7-(cyanomethyl)-7H-pyrrolo[2,3-d]pyrimidin-5-yl)phenyl)-3-(5-(tert-butyl)isoxazol-3-yl)urea (9ad). ¹H NMR (400 MHz, DMSO-*d*₆) δ : 9.54 (s, 1H), 8.94 (s, 1H), 8.24 (s, 1H), 7.58 (d, *J* = 7.4 Hz, 2H), 7.42 (d, *J* = 7.6 Hz, 2H), 7.38 (s, 1H), 6.53 (s, 1H), 6.26 (s, 2H), 5.41 (s, 2H), 1.31 (s, 9H). ¹³C NMR (101 MHz, DMSO-*d*₆) δ : 180.69, 158.85, 157.90, 152.72, 151.83, 150.70, 138.56, 129.41, 128.50, 122.66, 119.51, 117.08, 116.78, 100.62, 92.93, 32.94, 32.38, 28.82. HRMS (ESI), *m/z*: 431.1937 [M+H⁺].

1-(4-(4-amino-7-(2-cyanoethyl)-7H-pyrrolo[2,3-d]pyrimidin-5-yl)phenyl)-3-(5-(tert-butyl)isoxazol-3-yl)urea (9ae). ¹H NMR (400 MHz, DMSO-*d*₆) δ : 9.71 (s, 1H), 9.42 (s, 1H), 8.50 (s, 1H), 7.70 (s, 1H), 7.63 (d, *J* = 8.6 Hz, 2H), 7.42 (d, *J* = 8.5 Hz, 2H), 6.53 (s, 1H), 4.56 (t, *J* = 6.4 Hz, 2H), 3.19 (t, *J* = 6.4 Hz, 2H), 1.31 (s, 9H). ¹³C NMR (101 MHz, DMSO-*d*₆) δ : 180.57, 158.74, 152.03, 151.91, 148.02, 143.34, 139.41, 129.35, 126.41, 126.28, 119.33, 118.91, 118.78, 99.15, 92.97, 40.77, 32.94, 28.85, 18.82. HRMS (ESI), *m/z*: 445.2097 [M+H⁺].

General Procedures of Method B for the Syntheses of Compounds 13a-h

5-(4-amino-3-fluorophenyl)-7-tosyl-7H-pyrrolo[2,3-d]pyrimidin-4-amine (10). 4

(10.7 g, 25.8 mmol, 1 equiv) was dissolved in 1,4-dioxane/ethanol/water (v:v:v, 7:3:4, 200 ml) and treated with 4-amino-3-fluorobenzeneboronic acid pinacol ester (6.7 g, 28.4 mmol, 1.1 equiv), PdCl₂(dppf), and K₂CO₃ (7.1 g, 51.6 mmol, 2 equiv). The vial was sealed and heated with stirring at 80 °C for 2 h. The solvent was removed under reduced pressure to get the residue without purification.

5-(4-amino-3-fluorophenyl)-7H-pyrrolo[2,3-d]pyrimidin-4-amine (11). The crude production **10** was dissolved in water (100 mL) and KOH solid was added by proportion until pH was up to 14. After 1 h, the Ts group was removed completely. The mixture was quenched with water and extracted with CH₂Cl₂. The organic layer was separated and washed with saturated brine. After dried over Na₂SO₄, the solvent was removed under reduced pressure to afford the residue. The residue was dispersed in diethyl ether (50 mL) and stirred for 1 h. The residue was filtered and washed with diethyl ether to get **11** as gray solid. ¹H NMR (400 MHz, DMSO-*d*₆) δ : 11.66 (s, 1H), 8.08 (s, 1H), 7.11 (d, *J* = 2.1 Hz, 1H), 7.07 (dd, *J* = 12.5, 1.8 Hz, 1H), 6.98 (dd, *J* = 8.1, 1.8 Hz, 1H), 6.85 (dd, *J* = 9.5, 8.2 Hz, 1H), 5.99 (s, 2H), 5.21 (s, 2H).

To a mixture of **11** (243 mg, 1 mmol, 1 equiv) in CH₃CN was added Cs₂CO₃ (650 mg, 2 mmol, 2 equiv), followed by appropriate halide (1.2 mmol, 1.2 equiv). After reacting at 80 °C for 1 h, the mixture was filtered to remove salts and the filtrate was concentrated under reduced pressure to afford the crude **12a-h** without purification.

To a solution of intermediate **12a-h** (1 mmol, 1 equiv) in CH₃CN (20 mL) was added **8** (306 mg, 1 mmol, 1 equiv). After reaction at 80 °C for 1 h, a large amount of solid formed and the solid was obtained by filter and washed by diethyl ether. The corresponding crude **13a-h** wasn't purified further as off-white or pale yellow powder.

1-(4-(4-amino-7H-pyrrolo[2,3-d]pyrimidin-5-yl)-2-fluorophenyl)-3-(5-(tert-butyl)isoxazol-3-yl)urea (13a) ¹H NMR (400 MHz, DMSO-*d*₆) δ : 13.04 (s, 1H), 10.13 (s, 1H), 9.20 (s, 1H), 8.46 (s, 1H), 8.23 (t, *J* = 8.5 Hz, 1H), 7.61 (d, *J* = 2.3 Hz, 1H), 7.37 (dd, *J* = 12.0, 1.7 Hz, 1H), 7.27 (d, *J* = 8.4 Hz, 1H), 6.51 (s, 2H), 1.31 (s, 9H). ¹³C NMR (101 MHz, DMSO-*d*₆) δ : 180.78, 158.65, 153.91, 151.95, 151.74, 149.06, 142.92, 128.17, 126.74, 125.07, 124.38, 121.59, 118.03, 115.82, 98.84, 92.90, 32.96, 28.82. HRMS (ESI), *m/z*: 410.1734 [M+H⁺].

1-(4-(7-allyl-4-amino-7H-pyrrolo[2,3-d]pyrimidin-5-yl)-2-fluorophenyl)-3-(5-(tert-butyl)isoxazol-3-yl)urea (13b) ¹H NMR (400 MHz, DMSO-*d*₆) δ : 9.86 (s, 1H), 8.88 (s, 1H), 8.20 (t, *J* = 8.5 Hz, 1H), 8.16 (s, 1H), 7.33 (s, 1H), 7.33 (dd, *J* = 12.1, 1.8 Hz, 2H), 7.26 (dd, *J* = 8.5, 1.3 Hz, 1H), 6.51 (s, 1H), 6.19 (s, 2H), 6.05 (ddd, *J* = 22.5, 10.6, 5.5 Hz, 1H), 5.18 (dd, *J* = 10.2, 1.3 Hz, 1H), 5.09 (dd, *J* = 17.1, 1.4 Hz, 1H), 4.80 (d, *J* = 5.5 Hz, 2H), 1.31 (s, 9H). ¹³C NMR (101 MHz, DMSO-*d*₆) δ : 180.84, 158.69, 152.21, 151.59, 150.71, 134.51, 130.37, 125.86, 125.76, 124.83, 123.86, 121.48, 117.68, 115.50, 115.30, 114.70, 100.21, 92.83, 46.41, 32.95, 28.79. HRMS (ESI), *m/z*: 450.2042 [M+H⁺].

1-(4-(4-amino-7-(but-3-en-1-yl)-7H-pyrrolo[2,3-d]pyrimidin-5-yl)-2-fluorophenyl

)-3-(5-(tert-butyl)isoxazol-3-yl)urea (13c) ^1H NMR (400 MHz, $\text{DMSO-}d_6$) δ : 10.05 (s, 1H), 9.12 (s, 1H), 8.49 (s, 1H), 8.25 (t, $J = 8.5$ Hz, 1H), 7.73 (s, 1H), 7.36 (dd, $J = 12.0, 1.7$ Hz, 1H), 7.26 (d, $J = 8.4$ Hz, 1H), 6.51 (s, 1H), 5.80 (ddt, $J = 17.0, 10.3, 6.7$ Hz, 1H), 5.10 – 4.99 (m, 2H), 4.34 (t, $J = 7.0$ Hz, 2H), 2.61 (q, $J = 6.8$ Hz, 2H), 1.31 (s, 9H). ^{13}C NMR (101 MHz, $\text{DMSO-}d_6$) δ : 180.76, 158.64, 153.93, 151.84, 151.51, 147.91, 143.06, 134.96, 127.77, 127.26, 126.75, 124.97, 121.66, 118.06, 117.28, 115.74, 98.85, 92.91, 44.38, 34.21, 32.95, 28.83. HRMS (ESI), m/z : 464.2212 $[\text{M}+\text{H}^+]$.

1-(4-(4-amino-7-(prop-2-yn-1-yl)-7H-pyrrolo[2,3-*d*]pyrimidin-5-yl)-2-fluorophenyl)-3-(5-(tert-butyl)isoxazol-3-yl)urea (13d) ^1H NMR (400 MHz, $\text{DMSO-}d_6$) δ : 10.01 (s, 1H), 9.08 (s, 1H), 8.52 (s, 1H), 8.26 (t, $J = 8.5$ Hz, 1H), 7.73 (s, 1H), 7.39 (dd, $J = 12.0, 1.8$ Hz, 1H), 7.30 – 7.25 (m, 1H), 6.51 (s, 1H), 5.16 (d, $J = 2.4$ Hz, 2H), 1.31 (s, 9H). ^{13}C NMR (101 MHz, $\text{DMSO-}d_6$) δ : 180.79, 158.62, 153.89, 151.89, 151.72, 151.47, 147.62, 143.65, 139.19, 126.44, 125.07, 121.60, 117.95, 115.84, 99.28, 92.90, 78.45, 76.90, 34.64, 32.95, 28.82. HRMS (ESI), m/z : 448.1891 $[\text{M}+\text{H}^+]$.

1-(4-(4-amino-7-(2-methoxyethyl)-7H-pyrrolo[2,3-*d*]pyrimidin-5-yl)-2-fluorophenyl)-3-(5-(tert-butyl)isoxazol-3-yl)urea (13e) ^1H NMR (400 MHz, $\text{DMSO-}d_6$) δ : 10.10 (s, 1H), 9.16 (s, 1H), 8.51 (s, 1H), 8.25 (t, $J = 8.5$ Hz, 1H), 7.70 (s, 1H), 7.43 – 7.33 (m, 1H), 7.26 (m, 1H), 6.51 (s, 1H), 4.43 (t, $J = 5.1$ Hz, 2H), 3.76 (t, $J = 5.3$ Hz, 2H), 1.31 (s, 9H). ^{13}C NMR (101 MHz, $\text{DMSO-}d_6$) δ : 180.76, 158.64, 151.78, 148.04, 142.86, 129.36, 128.67, 127.52, 124.98, 121.68, 117.36, 115.77, 115.58, 98.89, 92.91, 70.54, 58.44, 45.73, 32.96, 28.83, 8.89. HRMS (ESI), m/z : 468.2159 $[\text{M}+\text{H}^+]$.

1-(4-(4-amino-7-(2-methoxyethyl)-7H-pyrrolo[2,3-d]pyrimidin-5-yl)-2-fluorophenyl)-3-(5-(tert-butyl)isoxazol-3-yl)urea (13f) ¹H NMR (400 MHz, DMSO-*d*₆) δ : 10.02 (s, 1H), 9.09 (s, 1H), 8.48 (s, 1H), 8.26 (t, *J* = 8.5 Hz, 1H), 7.68 (s, 1H), 7.37 (dd, *J* = 12.0, 1.8 Hz, 1H), 7.27 (d, *J* = 8.5 Hz, 1H), 6.51 (s, 1H), 4.42 (t, *J* = 5.3 Hz, 2H), 3.78 (t, *J* = 5.3 Hz, 2H), 3.46 (dd, *J* = 14.0, 7.0 Hz, 2H), 1.31 (s, 9H), 1.06 (t, *J* = 7.0 Hz, 3H). ¹³C NMR (101 MHz, DMSO-*d*₆) δ : 180.77, 158.64, 153.93, 151.51, 148.10, 143.07, 127.49, 126.87, 124.98, 121.66, 117.27, 115.61, 98.92, 92.90, 68.42, 65.83, 44.91, 32.96, 28.82, 15.42. HRMS (ESI), *m/z*: 482.2313 [M+H⁺].

1-(4-(4-amino-7-(cyanomethyl)-7H-pyrrolo[2,3-d]pyrimidin-5-yl)-2-fluorophenyl)-3-(5-(tert-butyl)isoxazol-3-yl)urea (13g) ¹H NMR (400 MHz, DMSO-*d*₆) δ : 10.10 (s, 1H), 9.16 (s, 1H), 8.57 (s, 1H), 8.26 (t, *J* = 8.5 Hz, 1H), 7.72 (s, 1H), 7.39 (dd, *J* = 11.9, 1.8 Hz, 1H), 7.28 (d, *J* = 8.4 Hz, 1H), 6.51 (s, 1H), 5.55 (s, 2H), 1.31 (s, 9H). ¹³C NMR (101 MHz, DMSO-*d*₆) δ : 180.77, 158.63, 153.91, 152.52, 148.27, 144.75, 127.23, 127.18, 127.07, 126.24, 125.07, 121.67, 118.30, 116.12, 115.87, 115.67, 99.82, 92.91, 32.96, 28.83. HRMS (ESI), *m/z*: 449.1848 [M+H⁺].

1-(4-(4-amino-7-(2-cyanoethyl)-7H-pyrrolo[2,3-d]pyrimidin-5-yl)-2-fluorophenyl)-3-(5-(tert-butyl)isoxazol-3-yl)urea (13h) ¹H NMR (400 MHz, DMSO-*d*₆) δ : 10.05 (s, 1H), 9.12 (s, 1H), 8.54 (s, 1H), 8.28 (t, *J* = 8.5 Hz, 1H), 7.79 (s, 1H), 7.65 (s, 1H), 7.37 (dd, *J* = 11.9, 1.8 Hz, 1H), 7.28 (d, *J* = 8.5 Hz, 1H), 6.51 (s, 1H), 4.60 – 4.51 (t, *J* = 6.5 Hz, 2H), 3.19 (t, *J* = 6.6 Hz, 2H), 1.31 (s, 9H). ¹³C NMR (101 MHz, DMSO-*d*₆) δ : 180.72, 158.64, 153.97, 151.86, 151.55, 148.04, 143.14, 142.99, 127.38, 126.92, 126.48, 125.25, 121.76, 118.76, 117.87, 115.75, 99.12, 92.94, 32.95, 28.83, 18.81.

HRMS (ESI), m/z : 463.2004 $[M+H^+]$.

Associated Contents

Supporting Information

Table S1 listing binding affinities of **9u** with more than 400 protein kinases; Table S2 listing IC_{50} values of compounds **9a-ae** and **13a-h** in RS4;11 cell; Table S3 listing inhibitory rate of compounds **9a-ae** and **13a-h** in HL-60 Cell; Table S4 listing IC_{50} values against hit target kinases of **9u**; Figure S1 listing the predicted bioavailability radar chart of the selected compounds; Figure S2 listing predicted boiled-egg plot of the selected compounds.

Biological assay methods: 1): Anti-proliferative assays; 2): Kinase profile assay and IC_{50} test; 3): Dissociation constants (K_d) assay for FLT3 mutants; 4): Western blotting of signaling pathways; 5): Cell cycle progression experiment; 6): Annexin V-FITC/PI apoptosis assay; 7): Pharmacokinetic study; 8): Molecular docking study; 9): Animal tumor models and treatment.

Molecular formula strings (CSV)

PDB code 4XUF was used for modeling docking in FLT3 of compounds CHMFL-FLT3-213, **9a**, **9b**, **9u**, and **13a**. Authors will release the Atomic Coordinates and experimental data upon article publication.

Author Contributions

The manuscript was written through contributions of all authors. All authors have given approval to the final version of the manuscript. X.Y., Y.C., W.H.Z., and J.H. contributed equally.

Notes

The authors declare no competing financial interest.

Corresponding Author Information:

*Lijuan Chen. Tel: +86-28-85164063; E-mail address: chenlijuan125@163.com.

*Haoyu Ye. E-mail address: haoyu_ye@scu.edu.cn.

ORCID ID

Lijuan Chen: 0000-0002-8076-163X

Acknowledgement

The authors greatly appreciate the financial support from Drug Innovation Major Project (2018ZX09711001-002-012), National Natural Science Foundation of China (81702991 and 81874297), and 1.3.5 project for disciplines of excellence, West China Hospital, Sichuan University.

Abbreviations Used:

FLT3, Fms-like tyrosine receptor kinase 3; ITD, internal tandem duplications; TKD, tyrosine kinase domain; RTK, receptor tyrosine kinases; K_d , dissociation constant; MTT, 3-(4,5-dimethylthiazol-2-yl)-2,5-diphenyltetrazolium bromide.

References

1. Seipel, K.; Marques, M. A. T.; Sidler, C.; Mueller, B. U.; Pabst, T. MDM2- and FLT3-inhibitors in the treatment of FLT3-ITD acute myeloid leukemia, specificity and efficacy of NVP-HDM201 and midostaurin. *Haematologica* **2018**, *103*, 1862-1872.
2. Lee, H. K.; Kim, H. W.; Lee, I. Y.; Lee, J.; Lee, J.; Jung, D. S.; Lee, S. Y.; Park, S. H.; Hwang, H.; Choi, J.-S.; Jung-Ho, Kim, S. W. K.; Kim, J. K.; Cools, J.; Koh, J. S.; Song, Ho-Juhn. G-749, a novel FLT3 kinase inhibitor, can overcome drug resistance for the treatment of acute myeloid leukemia. *Blood* **2014**, *123*, 2209-2219.
3. Chao, Q.; Sprankle, K. G.; Grotzfeld, R. M.; Lai, A. G.; Carter, T. A.; Velasco, A. M.; Gunawardane, R. N.; Cramer, M. D.; Gardner, M. F.; James, J.; Zarrinkar, P. P.; Patel, H. K.; Bhagwat, S. S. Identification of N-(5-tert-butyl-isoxazol-3-yl)-N-{4-[7-(2-morpholin-4-yl-ethoxy)imidazo[2,1-b][1,3]benzothiazol-2-yl]phenyl}urea dihydrochloride (AC220), a uniquely potent, selective, and efficacious FMS-like tyrosine kinase-3 (FLT3) inhibitor. *J. Med. Chem.* **2009**, *52*, 7808-7816.
4. Larrosa-Garcia, M.; Baer, M. R. FLT3 inhibitors in acute myeloid leukemia: current status and future directions. *Mol. Cancer. Ther.* **2017**, *16*, 991-1001.
5. Gilliland, D. G.; Griffin, J. D. The roles of FLT3 in hematopoiesis and leukemia. *Blood* **2002**, *100*, 1532-1542.
6. Frohling, S.; Schlenk, R. F.; Breitruck, J.; Benner, A.; Kreitmeier, S.; Tobis, K.; Dohner, H.; Dohner, K.; leukemia, A. M. L. S. G. U. A. m. Prognostic significance of

activating FLT3 mutations in younger adults (16 to 60 years) with acute myeloid leukemia and normal cytogenetics: a study of the AML Study Group Ulm. *Blood* **2002**, *100*, 4372-4380.

7. Maifrede, S.; Nieborowska-Skorska, M.; Sullivan-Reed, K.; Dasgupta, Y.; Podszywalow-Bartnicka, P.; Le, B. V.; Solecka, M.; Lian, Z.; Belyaeva, E. A.; Nersesyan, A.; Machnicki, M. M.; Toma, M.; Chatain, N.; Rydzanicz, M.; Zhao, H.; Jelinek, J.; Piwocka, K.; Sliwinski, T.; Stoklosa, T.; Ploski, R.; Fischer, T.; Sykes, S. M.; Koschmieder, S.; Bullinger, L.; Valent, P.; Wasik, M. A.; Huang, J.; Skorski, T. Tyrosine kinase inhibitor-induced defects in DNA repair sensitize FLT3(ITD)-positive leukemia cells to PARP1 inhibitors. *Blood* **2018**, *132*, 67-77.

8. Bacher, U.; Haferlach, C.; Kern, W.; Haferlach, T.; Schnittger, S. Prognostic relevance of FLT3-TKD mutations in AML: the combination matters-an analysis of 3082 patients. *Blood* **2007**, *111*, 2527-2537.

9. Shabbir, M.; Stuart, R. Lestaurtinib, a multitargeted tyrosine kinase inhibitor: from bench to bedside. *Expert. Opin. Investig. Drugs* **2010**, *19*, 427-436.

10. Schlenk RF.; Kayser. S.. Midostaurin: a multiple tyrosine kinases inhibitor in acute myeloid leukemia and systemic mastocytosis. *Recent Results Cancer Res.* **2018**, *212*, 199-214.

11. Wilhelm, S. M.; Adnane, L.; Newell, P.; Villanueva, A.; Llovet, J. M.; Lynch, M. Preclinical overview of sorafenib, a multikinase inhibitor that targets both Raf and VEGF and PDGF receptor tyrosine kinase signaling. *Mol. Cancer Ther.* **2008**, *7*, 3129-3140.

12. Levis, M. Midostaurin approved for FLT3-mutated AML. *Blood* **2017**, *129*, 3403-3406.
13. Lusk, M. R.; DeAngelo, D. J. Midostaurin/PKC412 for the treatment of newly diagnosed FLT3 mutation-positive acute myeloid leukemia. *Expert Rev. Hematol.* **2017**, *10*, 1033-1045.
14. Kim, E. S. Midostaurin: first global approval. *Drugs* **2017**, *77*, 1251-1259.
15. Smith, C. C.; Wang, Q.; Chin, C. S.; Salerno, S.; Damon, L. E.; Levis, M. J.; Perl, A. E.; Travers, K. J.; Wang, S.; Hunt, J. P.; Zarrinkar, P. P.; Schadt, E. E.; Kasarskis, A.; Kuriyan, J.; Shah, N. P. Validation of ITD mutations in FLT3 as a therapeutic target in human acute myeloid leukaemia. *Nature* **2012**, *485*, 260-263.
16. Wang, A.; Li, X.; Chen, C.; Wu, H.; Qi, Z.; Hu, C.; Yu, K.; Wu, J.; Liu, J.; Liu, X.; Hu, Z.; Wang, W.; Wang, W.; Wang, W.; Wang, L.; Wang, B.; Liu, Q.; Li, L.; Ge, J.; Ren, T.; Zhang, S.; Xia, R.; Liu, J.; Liu, Q. Discovery of 1-(4-(4-Amino-3-(4-(2-morpholinoethoxy)phenyl)-1H-pyrazolo[3,4-*d*]pyrimidin-1-yl)phenyl)-3-(5-(tert-butyl)isoxazol-3-yl)urea (CHMFL-FLT3-213) as a highly potent type II FLT3 kinase inhibitor capable of overcoming a variety of FLT3 kinase mutants in FLT3-ITD positive AML. *J. Med. Chem.* **2017**, *60*, 8407-8424.
17. Takeshi Yamaura; Toshiyuki N.; Ken Uda; Hayato Ogura; Wiyon Shin; Naoya K.; Koichi Saito; Norie Fujikawa; Tomomi Date; Masaru Takasaki; Daisuke T.; Atsushi Hirai; Akimi Akashi; Fangli Chen; Yoshiya Adachi; Yuichi I.; Fumihiko Hayakawa; Shinji Hagiwara; Tomoki Naoe; Hitoshi Kiyoi. A novel irreversible FLT3 inhibitor, FF-10101, shows excellent efficacy against AML cells with FLT3

1
2
3
4 mutations. *Blood* **2018**, *131*, 426-438.

5
6
7 18. Levis, M. Quizartinib for the treatment of FLT3/ITD acute myeloid leukemia.
8
9 *Future Oncol.* **2014**, *10*, 1571-1579.

10
11
12 19. Wu, H.; Wang, A.; Qi, Z.; Li, X.; Chen, C.; Yu, K.; Zou, F.; Hu, C.; Wang, W.;
13
14 Zhao, Z.; Wu, J.; Liu, J.; Liu, X.; Wang, L.; Wang, W.; Zhang, S.; Stone, R. M.;
15
16 Galinsky, I. A.; Griffin, J. D.; Weinstock, D.; Christodoulou, A.; Wang, H.; Shen, Y.;
17
18 Zhai, Z.; Weisberg, E. L.; Liu, J.; Liu, Q. Discovery of a highly potent FLT3 kinase
19
20 inhibitor for FLT3-ITD-positive AML. *Leukemia* **2016**, *30*, 2112-2116.
21
22

23
24
25 20. Alexander A Warkentin; Michael S Lopez; Elisabeth A Lasater; Kimberly Lin;
26
27 Bai-Liang He; Anskar YH Leung; Catherine C Smith; Neil P Shah; Shokat, K. M.
28
29 Overcoming myelosuppression due to synthetic lethal toxicity for FLT3-targeted
30
31 acute myeloid leukemia therapy. *eLife* **2014**, *3*, e03445.
32
33

34
35 21. Zarrinkar, P. P.; Gunawardane, R. N.; Cramer, M. D.; Gardner, M. F.; Brigham,
36
37 D.; Belli, B.; Karaman, M. W.; Pratz, K. W.; Pallares, G.; Chao, Q.; Sprankle, K. G.;
38
39 Patel, H. K.; Levis, M.; Armstrong, R. C.; James, J.; Bhagwat, S. S. AC220 is a
40
41 uniquely potent and selective inhibitor of FLT3 for the treatment of acute myeloid
42
43 leukemia (AML). *Blood* **2009**, *114*, 2984-2892.
44
45

46
47
48 22. Li, X.; Wang, A.; Yu, K.; Qi, Z.; Chen, C.; Wang, W.; Hu, C.; Wu, H.; Wu, J.;
49
50 Zhao, Z.; Liu, J.; Zou, F.; Wang, L.; Wang, B.; Wang, W.; Zhang, S.; Liu, J.; Liu, Q.
51
52 Discovery of (R)-1-(3-(4-Amino-3-(4-phenoxyphenyl)-1H-pyrazolo[3,4-d]pyrimidin-
53
54 1-yl)piperidin-1-yl)-2-(dimethylamino)ethanone (CHMFL-FLT3-122) as a potent and
55
56 orally available FLT3 kinase inhibitor for FLT3-ITD positive acute myeloid
57
58
59
60

leukemia. *J. Med. Chem.* **2015**, *58*, 9625-9638.

23. Liang, X.; Wang, B.; Chen, C.; Wang, A.; Hu, C.; Zou, F.; Yu, K.; Liu, Q.; Li, F.; Hu, Z.; Lu, T.; Wang, J.; Wang, L.; Weisberg, E.; Li, L.; Xia, R.; Wang, W.; Ren, T.; Ge, J.; Liu, J.; Liu, Q. Discovery of N-(4-(6-acetamidopyrimidin-4-yloxy)phenyl)-2-(2-(trifluoromethyl)phenyl)acetamide (CHMFL-FLT3-335) as a potent Fms-like tyrosine kinase 3 internal tandem duplications (FLT3-ITD) mutant selective inhibitor for acute myeloid leukemia. *J. Med. Chem.* **2019**, *62*, 875–892.

24. Li, G. B.; Ma, S.; Yang, L. L.; Ji, S.; Fang, Z.; Zhang, G.; Wang, L. J.; Zhong, J. M.; Xiong, Y.; Wang, J. H.; Huang, S. Z.; Li, L. L.; Xiang, R.; Niu, D.; Chen, Y. C.; Yang, S. Y. Drug discovery against psoriasis: identification of a new potent FMS-like tyrosine kinase 3 (FLT3) inhibitor, 1-(4-((1H-pyrazolo[3,4-d]pyrimidin-4-yl)oxy)-3-fluorophenyl)-3-(5-(tert-butyl)isoxazol-3-yl)urea, that showed potent activity in a psoriatic animal model. *J. Med. Chem.* **2016**, *59*, 8293-8305.

25. Burslem, G. M.; Song, J.; Chen, X.; Hines, J.; Crews, C. M. Enhancing antiproliferative activity and selectivity of a FLT-3 inhibitor by proteolysis targeting chimera conversion. *J. Am. Chem. Soc.* **2018**, *140*, 16428-16432.

26. Gillis, E. P.; Eastman, K. J.; Hill, M. D.; Donnelly, D. J.; Meanwell, N. A. Applications of fluorine in medicinal chemistry. *J. Med. Chem.* **2015**, *58*, 8315-8359.

27. Weisel, K. C.; Yildirim, S.; Schweikle, E.; Kanz, L.; Mohle, R. Effect of FLT3 inhibition on normal hematopoietic progenitor cells. *Ann. N. Y. Acad. Sci.* **2007**, *1106*, 190-196.

28. Ghiaur, G.; Levis, M. Mechanisms of resistance to FLT3 inhibitors and the role

- of the bone marrow microenvironment. *Hematol. Oncol. Clin. North. Am.* **2017**, *31*, 681-692.
29. Smith, C. C.; Lasater, E. A.; Lin, K. C.; Wang, Q.; McCreery, M. Q.; Stewart, W. K.; Damon, L. E.; Perl, A. E.; Jeschke, G. R.; Sugita, M.; Carroll, M.; Kogan, S. C.; Kuriyan, J.; Shah, N. P. Crenolanib is a selective type I pan-FLT3 inhibitor. *Proc. Natl. Acad. Sci. U. S. A.* **2014**, *111*, 5319-5324.
30. Kesarwani, M.; Huber, E.; Azam, M. Overcoming AC220 resistance of FLT3-ITD by SAR302503. *Blood Cancer J.* **2013**, *3*, e138.
31. Daina, A.; Michielin, O.; Zoete, V. SwissADME: a free web tool to evaluate pharmacokinetics, drug-likeness and medicinal chemistry friendliness of small molecules. *Sci. Rep.* **2017**, *7*, 42717.
32. Sun, D.; Yang, Y.; Lyu, J.; Zhou, W.; Song, W.; Zhao, Z.; Chen, Z.; Xu, Y.; Li, H. Discovery and rational design of pteridin-7(8H)-one-based inhibitors targeting FMS-like tyrosine kinase 3 (FLT3) and its mutants. *J. Med. Chem.* **2016**, *59*, 6187-6200.
33. Roversi, F. M.; Pericole, F. V.; Machado-Neto, J. A.; da Silva Santos Duarte, A.; Longhini, A. L.; Corrocher, F. A.; Palodetto, B.; Ferro, K. P.; Rosa, R. G.; Baratti, M. O.; Verjovski-Almeida, S.; Traina, F.; Molinari, A.; Botta, M.; Saad, S. T. Hematopoietic cell kinase (HCK) is a potential therapeutic target for dysplastic and leukemic cells due to integration of erythropoietin/PI3K pathway and regulation of erythropoiesis: HCK in erythropoietin/PI3K pathway. *Biochim. Biophys. Acta. Mol. Basis. Dis.* **2017**, *1863*, 450-461.

34. S Rudat; A. P.; YY Cheng; J Holtmann; JM Ellegast; C Bühler; D Di Marcantonio; E Martinez; S Göllner; C Wickenhauser; C Müller-Tidow; C Lutz; L Bullinger; MD Milson; SM Sykes; S Fröhling; C Scholl. RET-mediated autophagy suppression as targetable co-dependence in acute myeloid leukemia. *Leukemia* **2018**, 32, 2189-2202.
35. Iriyama, N.; Yuan, B.; Hatta, Y.; Takagi, N.; Takei, M. Lyn, a tyrosine kinase closely linked to the differentiation status of primary acute myeloid leukemia blasts, associates with negative regulation of all-trans retinoic acid (ATRA) and dihydroxyvitamin D3 (VD3)-induced HL-60 cells differentiation. *Cancer Cell Int.* **2016**, 16, 37.
36. Serafin, V.; Capuzzo, G.; Milani, G.; Minuzzo, S. A.; Pinazza, M.; Bortolozzi, R.; Bresolin, S.; Porcu, E.; Frasson, C.; Indraccolo, S.; Basso, G.; Accordi, B. Glucocorticoid resistance is reverted by LCK inhibition in pediatric T-cell acute lymphoblastic leukemia. *Blood* **2017**, 130, 2750-2761.
37. Sarah Krause; Christian Pfeiffer; Susanne Strube; Ameera Alsadeq; Henning Fedders; Christian Vokuhl; Sonja Loges; Jonas Waizenegger; Isable Ben-Batalla; Gunnar Cario; Anja M.; Martin Schrappe; and; Denis M. Schewe. Mer tyrosine kinase promotes the survival of t(1;19)-positive acute lymphoblastic leukemia (ALL) in the central nervous system (CNS). *Blood* **2015**, 125, 820-830.
38. Masanobu Tsubaki1; Tomoya T.; Toshiki Kino, Kazuko Sakai; Tatsuki Itoh; Motohiro Imano; Takashi. N.; Kazuto Nishio; Takao Satou; and Shozo Nishida. Contributions of MET activation to BCR-ABL1 tyrosine kinase inhibitor resistance in

chronic myeloid leukemia cells. *Oncotarget* **2017**, *8*, 38717-38730.

39. Bachegowda, L.; Morrone, K.; Winski, S. L.; Mantzaris, I.; Bartenstein, M.; Ramachandra, N.; Giricz, O.; Sukrithan, V.; Nwankwo, G.; Shahnaz, S.; Bhagat, T.; Bhattacharyya, S.; Assal, A.; Shastri, A.; Gordon-Mitchell, S.; Pellagatti, A.; Boultonwood, J.; Schinke, C.; Yu, Y.; Guha, C.; Rizzi, J.; Garrus, J.; Brown, S.; Wollenberg, L.; Hogeland, G.; Wright, D.; Munson, M.; Rodriguez, M.; Gross, S.; Chantry, D.; Zou, Y.; Plataniias, L.; Burgess, L. E.; Pradhan, K.; Steidl, U.; Verma, A. Pexmetinib: a novel dual inhibitor of Tie2 and p38 MAPK with efficacy in preclinical models of myelodysplastic syndromes and acute myeloid leukemia. *Cancer Res.* **2016**, *76*, 4841-4849.

40. Elina Armstrong; Satu. V.; Juha Partanen; Jaana Korhonen; and Rutta Alitalo. Expression of fibroblast growth factor receptors in human leukemia cells. *Cancer Res.* **1992**, *52*, 2004-2007.

41. Porta, R.; Borea, R.; Coelho, A.; Khan, S.; Araujo, A.; Reclusa, P.; Franchina, T.; Van Der Steen, N.; Van Dam, P.; Ferri, J.; Sirera, R.; Naing, A.; Hong, D.; Rolfo, C. FGFR a promising druggable target in cancer: Molecular biology and new drugs. *Crit. Rev. Oncol. Hematol.* **2017**, *113*, 256-267.

42. Zhang, W.; DeRyckere, D.; Hunter, D.; Liu, J.; Stashko, M. A.; Minson, K. A.; Cummings, C. T.; Lee, M.; Glaros, T. G.; Newton, D. L.; Sather, S.; Zhang, D.; Kireev, D.; Janzen, W. P.; Earp, H. S.; Graham, D. K.; Frye, S. V.; Wang, X. UNC2025, a potent and orally bioavailable MER/FLT3 dual inhibitor. *J. Med. Chem.* **2014**, *57*, 7031-7041.

43. Heinrich, M. C.; Griffith, D.; McKinley, A.; Patterson, J.; Presnell, A.; Ramachandran, A.; Debiec-Rychter, M. Crenolanib inhibits the drug-resistant PDGFRA D842V mutation associated with imatinib-resistant gastrointestinal stromal tumors. *Clin. Cancer Res.* **2012**, *18*, 4375-4384.
44. Gupta, P.; Kathawala, R. J.; Wei, L.; Wang, F.; Wang, X.; Druker, B. J.; Fu, L. W.; Chen, Z. S. PBA2, a novel inhibitor of imatinib-resistant BCR-ABL T315I mutation in chronic myeloid leukemia. *Cancer Lett.* **2016**, *383*, 220-229.
45. Gucky, T.; Reznickova, E.; Radosova Muchova, T.; Jorda, R.; Klejova, Z.; Malinkova, V.; Berka, K.; Bazgier, V.; Ajani, H.; Lepsik, M.; Divoky, V.; Krystof, V. Discovery of N²-(4-Amino-cyclohexyl)-9-cyclopentyl-N⁶-(4-morpholin-4-ylmethyl-phenyl)-9H-purine-2,6-diamine as a potent FLT3 kinase inhibitor for acute myeloid leukemia with FLT3 mutations. *J. Med. Chem.* **2018**, *61*, 3855-3869.
46. Yeung, J.; Esposito, M. T.; Gandillet, A.; Zeisig, B. B.; Griessinger, E.; Bonnet, D.; So, C. W. beta-Catenin mediates the establishment and drug resistance of MLL leukemic stem cells. *Cancer cell* **2010**, *18*, 606-618
47. Julie A. Zorn; Qi Wang; Eric Fujimura; Tiago Barros; John Kuriyan. Crystal structure of the FLT3 kinase domain bound to the inhibitor quizartinib (AC220). *PLoS One* **2015**, *10*, e0121177.

Table of Contents Graphic

FLT3 IC_{50} : 7 nM

FLT3 vs c-Kit: > 40-fold

MV4-11 IC_{50} : 0.089 nM

Molm-13 IC_{50} : 0.022 nM

F% : 59.5%

TGI: (Molm-13, 3 mg/kg po) 94.5%

TGI: (MV4-11, 10 mg/kg po) 100%

